since 1961

Baltica

BALTICA Volume 39 Number 1 June 2026: 81–102
https://doi.org/10.5200/baltica.2026.1.8

Research article

A comprehensive assessment of differences in rock mass classes estimated during investigation and encountered during tunnel excavation

Recep Temiz, Ebu Bekir Aygar, Candan Gokceoglu*

Temiz, R., Aygar, E.B., Gokceoglu, C. 2026. A comprehensive assessment of differences in rock mass classes estimated during investigation and encountered during tunnel excavation. *Baltica 39 (1)*, 81–102. Vilnius. ISSN 0067-3064.
Manuscript submitted 23 September 2025 /Accepted 2 April 2026 / Available online 7 May 2026

Abstract. The present study aims to perform statistical analyses on rock mass class differences estimated during the investigation and encountered during excavation phases of various tunnel projects and to quantitatively evaluate these differences. Using data obtained from 14 different highway tunnels constructed in Türkiye, the differences between the rock mass classes predicted during the investigation phase and the actual values encountered during excavation were analyzed with the parameter of Mean Percentage Absolute Difference (MPAD). The effects of the parameters introduced in the study, such as the drilling length ratio to tunnel length (LDn), total core recovery ratio (TCRn), rock quality designation ratio (RQDn) and uniaxial compressive strength test number ratio (UCSn), on these differences were investigated with regression and Random Forest algorithms. The results showed that TCRn and RQDn have a strong inverse relationship on MPAD, in other words, the rock mass class differences decrease with the increase of these parameters. In addition, it was determined that the drilling length and total core recovery values are of critical importance in reducing the uncertainties in the tunnel route. This study is expected to contribute to more accurate predictions and to reduce cost and time losses by providing a quantitative approach to minimize uncertainties in tunnel constructions during the excavation phase.

Keywords: *geotechnical investigation; drilling, tunnel; RQD; RMR; uncertainty*

Recep Temiz (rtemiz@kgm.gov.tr), https://orcid.org/0009000974007997;
General Directorate of Highways, 06420, Çankaya, Ankara, Türkiye;
Ebu Bekir Aygar (aygar@igtunnel.com), https://orcid.org/0009000858522414;
IG Tunnel Engineering Consulting Company, 06640, Çankaya, Ankara, Türkiye;
Candan Gokceoglu (candan.gokceoglu@kapadokya.edu.tr), https://orcid.org/0000000347629933;*
Cappadocia University, Faculty of Computer and Information Technologies, 50420 Mustafapasa, Urgup, Nevsehir, Türkiye
**Corresponding author*

INTRODUCTION

One of the most iconic statements for rock environments was published by Goodman (1995) with the words "when the materials are natural rock, the only thing known with certainty is that this material will never be known with certainty," and although important scientific and technological advances occurred, this statement still retains significant validity. According to Spross *et al*. (2020), rock engineering design must be viewed as decision-making under uncertainty and they proposed a framework making the design process subject to general risk management principles, as risk is defined as "effect of uncertainties on objectives". Benardos and Kaliampakos (2017) stated that as demand for the development of new underground structures, regardless of the ground conditions, has increased, safety and risk considerations have become even more important. A framework proposed by Miranda *et al*. (2009) is applied to the case of deformability modulus updating in a large underground structure to quantify uncertainty, while Pandit *et al*. (2019) employed a probabilistic approach to characterize rock mass using limited laboratory tests

and field data for the stability analysis of rock slopes and tunnels.

A tunnel is a linear engineering structure, and during its excavation and construction, environments with different geological and geotechnical properties are encountered. Before excavation works, drillings are performed to determine the geological and geotechnical properties of the tunnel route. In addition, surface investigation is combined with data obtained from drilling and geophysical measurements to predict the underground route properties. Using the data obtained from these investigations, the excavation method and the preliminary support system design are determined. In tunnel construction, construction time and costs are controlled by the excavation method and the support system. Therefore, the adequacy of the geological and geotechnical data of the tunnel route obtained during the investigation phase, in terms of quality and quantity, is of vital importance for a tunnel project. In some cases, tunnel routes can be hundreds of meters below the surface, and in mountainous areas, accessing the tunnel route from the surface may be impossible. This can significantly hinder surface drilling and geophysical studies. However, although important advancements over the recent years in computer methods and artificial intelligence algorithms for analyzing and synthesizing exploration and site investigation geological data for design purposes, which should have decreased project risk, unexpected failures and construction problems still occur (Carter, Barnett 2022). Carter and Barnett (2022) stated that part of this diminished appreciation of structural geological controls on rock mass behaviour are likely to be attributed to an inappropriate use of computational geostatistics, block modelling and geomechanics computer codes, without a significant structural geological input. Consequently, a significant structural geological input is the key for a realistic geological-geotechnical model, and these inputs are obtained from sufficient drillings along tunnel runnel route.

Undoubtedly, the adequacy of the amount of data and the complexity of the geological environment directly affects the accuracy of these predictions. In other words, the more data there are and the more homogeneous the environment is, the more accurate the predictions become. However, the differences between the geological and geotechnical conditions that are often predicted and encountered during tunnel construction continue to be a problem. This problem generally arises from reasons such as incomplete geological and geotechnical investigations performed during the investigation phase while determining rock classes, the scarcity of drillings, incomplete and incorrect definitions carried out during the preparation of drilling logs, and the lack of in-situ or laboratory tests. Such deficiencies are carried out during the investigation phase and result in problems during the excavation phase. The T1 tunnel in the Ankara–Izmir High-Speed Railway project of Turkiye is the fastest construction among the tunnel boring machines tunnels with a diameter of 13 m and larger, and Karahan and Gokceoglu (2025) emphasized that the most important factor in this success is the accurate determination of geological and geotechnical conditions and taking the necessary precautions in advance. On the other hand, although it is the same size as the T1 tunnel, the tunnel boring machine in the T26 tunnel, which is part of the Ankara–Istanbul High-Speed Railway project, got stuck and lost its function, as a result of which the tunnel construction period was considerably extended. Gokceoglu *et al*. (2022) explained the main reasons for this failure as unexpected geological-geotechnical conditions and therefore the selection of an inappropriate tunnel boring machine. Seo *et al*. (2018) examined on the factors affecting the performance of tunnel boring machine in hard rock, and they stated that subjectivity in geological mapping is a substantial risk factor in the evaluation of the fracturing factor. The fracturing factor has a great effect on the estimation of net penetration rates used to estimate excavation times and costs for tunnel projects excavated with tunnel boring machines (Seo *et al*. 2018). In addition, Isaksson and Stille (2005) stated that numerous decisions have to be made regarding tender price and budget in the planning stage of tunnelling projects, and many studies presented that the predicted costs and time schedules are often exceeded in practice. However, a reliable geological model often allows providing an effective design and facing the construction phase without unpleasant surprises in tunnel projects (Perello 2011), and Perello (2011) stated that a geological model can be considered reliable when it is a valid support to correctly foresee the rock mass behaviour, therefore preventing unexpected events during the excavation. In Eurocode 7, reliability-based and the observational methods are suggested by Eurocode 7 for managing uncertainty in tunnel design. Reliability-based methods account for uncertainty by acknowledging the random variation of the input parameters while the observational method does this by verifying the expected behaviour from an initial design during the course of construction (Bjureland *et al*. 2017). A guidance described by Eurocode 7 is not given on the selection of suitable parameters for observation (Bjureland *et al*. 2017).

As stated in the literature given above, differences between the predicted and encountered rock classes along tunnel route cause unforeseen cost increases and increased construction time, and it is an important research subject in tunnel engineering. Preventing such uncertainties and minimizing the differences between the predicted and encountered rock classes

are one of the important goals in terms of tunnel engineering. In order to minimize this difference, the amount of investigation conducted and its assessment are important issues. The case studies presenting the tunnel failures in the literature is given in the subsequent section to show the importance of the study.

It is an important issue to reveal the reasons for this problem, which is frequently encountered both in scientific literature and in tunnel engineering practice and which ultimately causes a serious loss of construction time and economic losses. Consequently, the purpose of the present study is to assess the differences between the rock mass classes determined during investigation and excavation phases for tunnels. The results of the present study may help for decision-makers and engineers when determining the optimum amount of drilling, and may contribute to the tunnelling literature. In addition, the original data obtained from 14 different tunnel cases is presented in the study. For the purpose of the study, different tunnel data were used to describe the uncertainty, and the resulting differences were studied with statistical methods in terms of their relationships with various parameters introduced in this study. The obtained results were discussed, and it was revealed which parameters controlled the rock class differences between the investigation and construction stages.

PREVIOUS STUDIES

In tunnel projects, inadequate work during the investigation phase and unforeseen geological conditions during construction lead to both lost time and increased costs, negatively impacting project efficiency. Numerous studies exist in the literature addressing the problems encountered in tunnels due to unforeseen geological conditions. Some of these studies offer methodologies for minimizing unforeseen geological conditions and uncertainty in tunnels, while others address the problems encountered. Examples from these studies are discussed in detail below.

Fookes (1997) developed a method and flow diagram by presenting suggestions on the model encountered with the predicted geological model under the title of geology for engineers. Boyd *et al*. (2020) investigated the estimation of rock classes encountered before and during excavation for the Caldecott Tunnel using geostatistical methods and presented assessments on the sources of the differences. Dong *et al*. (2015) proposed a procedure for a 3D geotechnical model in order to reduce geological and geotechnical uncertainties especially under low overburden in urban tunnels in Aachen, Germany. Ertharter *et al*. (2023) proposed a ground model with Building Information Modelling (BIM) in the Angath Tunnel in Austria. It was stated that the development of the BIM ground model was necessary and had great benefits. Fang *et al*. (2024) investigated the uncertainties in tunnel risk estimation with seismic data. For this purpose, Fang *et al*. (2024) developed an innovative workflow and studied the geological changes in the advancement direction of the TBM with continuous seismic data. Fellin *et al*. (2010) presented suggestions for the stability and analysis of tunnel face stability of tunnels excavated in weak grounds with low overburden thickness, using laboratory tests and a finite element model. Fortsakis *et al*. (2012) investigated the anisotropic rock behaviour in tunnels excavated in bedded rock mass and concluded that this behaviour was within a wide range. Gangrade *et al*. (2022) investigated the void risk and grouting volume encountered during tunnel construction with a probabilistic approach. Gangrade *et al*. (2022) stated that there was a possibility of encountering voids especially in tunnels excavated in karstic units and estimated the injection amount to fill the voids with a probabilistic approach. Hack *et al*. (2006) performed a study on the development of a three-dimensional model for engineering geology. Hao *et al*. (2016, 2018) conducted risk assessment of water flow in karstic tunnels with uncertainty analysis. Li *et al*. (2021) investigated the unexpected conditions and uncertainties in rock tunnel engineering in their study. Madsen *et al*. (2022) developed a new probabilistic approach for 3D geological modelling, called geology-driven modelling (GDM). Mahmoodzadeh *et al*. (2021, 2022) studied to estimate tunnel geology, construction time and cost using machine learning methods. In these studies, Mahmoodzadeh *et al*. (2021 and 2022) used Gaussian Process Regression (GPR), Support Vector Regression (SVR), and Decision Tree (DT) methods and found that the GPR method provided the highest performance. Panthi and Nilsen (2007) investigated the squeezing mechanism in tunnels constructed in the Himalayas in Nepal, using uncertainty analysis and stated that the most important and difficult part of the squeezing mechanism is the determination of the strength of the rock mass. Sarma *et al*. (2022) studied to determine the locations of possible collapses in the tunnel using Tunnel Boring Machine (TBM) parameters and Rock Mass Rating (RMR) values with the help of Machine Learning (ML) model. Despite some deficiencies, Sarma *et al*. (2022) suggested that the ML model could be used in ongoing tunnel projects. Xiong *et al*. (2018) studied a 3D multi-scale geology model for risk assessment in tunnel engineering.

Merrie (2009) presented a case from the Singapore Circle Line project, noting that a sinkhole occurred in a tunnel with complex geology and that during the excavation phase a sinkhole was encountered in a section identified as granite by drilling. Therefore, Merrie (2009) emphasized the importance of a geological

interpretation process and an accurate geotechnical model during the investigation phase for tunnel safety. Li *et al*. (2010) emphasized that understanding the geology of a tunnel before boring is highly advantageous for the safety and efficiency of tunnel construction. The Qiyueshan Tunnel, located on the Hurongxi Highway in China, was constructed in an area with widespread karst formations (Li *et al*. 2010). The rocks surrounding the tunnel consist of highly soluble microcrystalline limestone, and the presence of underground rivers and karst caves increases the risk of water inrush during tunnel construction. This geological situation made it difficult to predict hazards such as karst caves and groundwater intrusion. During construction, especially during the rainy season, water intrusions occurred in the left side wall of the tunnel, causing a 500-meter section of the tunnel to be submerged (Li *et al*. 2010).

Alija *et al*. (2014) discuss the partial collapse of the Ampurdán Tunnel in Spain. The tunnel passes through a weak and weather-sensitive geological unit, the Ampurdán claystone formation. This unit is characterized by low strength and high deformation properties. While geotechnical investigations conducted prior to the project generally predicted the geotechnical properties, unexpected changes occurred during tunnel excavation (Alija *et al*. 2014). In particular, the rapid weathering of the claystone material due to post-excavation weathering and water infiltration led to the partial collapse of the tunnel (Alija *et al*. 2014). The Ceneri Base tunnel constructed between Bellinzona and Lugano as part of Switzerland's Alp-Transit Gotthard AG project emphasized the tunnel's complex geological conditions caused by unpredictable faults (Thum, De Paoli 2015). These unforeseen conditions controlled to stability issues during tunnel excavation, particularly wedge blocks falling from the roof and side walls (Thum, De Paoli 2015).

Ye *et al*. (2015) reported deformations of up to 0.8 meters around the tunnel during construction in Shanghai, China, in the Shanghai clays. Ye *et al*. (2015) determined that these deformations were much larger than expected due to the false application of the backfill grouting, TBM operational issues, and frictional effects between the ground and the machine during tunnel construction. Huang *et al*. (2016) presented that severe deformations occurred during the construction of a metro line constructed using a TBM in the Shanghai clays of China due to extreme surface loading (surcharge). These included openings at the joints of tunnel segments, failures of segment-connecting bolts, concrete cracks, and water leaks. These deformations resulted in the tunnel losing its water-proofing function and compromising its structural integrity (Huang *et al*. 2016).

Since the Kop Tunnel, located on the Erzurum-Bayburt- Gümüşhane road in Türkiye, is located at the intersection of the Eastern Anatolian and Northern Anatolian fault zones, certain problems such as excessive overbreakings, water and gas intrusions along the tunnel line during construction had an adverse impact on both the excavation work and the completion time of the work (Coruh *et al*. 2017). Liu *et al*. (2020) reported that serious structural problems arose during the construction of a subway line in the Shanghai clays in China due to ground settlements and leaks. In particular, differential settlement occurred between tunnel segments and displacement at the circumferential joints. This resulted in cracking and spalling of the concrete lining. The main cause of the problem was identified as water and soil loss in the subgrade. These losses reduced the reaction pressure beneath the tunnel and caused the tunnel to settle (Liu *et al*. 2020). The tunnels constructed in South Korea under complex geological conditions and the effects of natural hazards such as extreme rainfall, floods, and strong winds encountered adverse impacts such as collapses, landslides, and floods during tunnel construction (Yum *et al*. 2020). However, strong winds and heavy rainfall, particularly those caused by typhoons, caused significant financial losses during construction. These problems led to unexpected cost increases and lost time in construction projects (Yum *et al*. 2020).

Aygar and Gokceoglu (2020) presented that a fault defined as a crushed zone and a low-strength and plastic clay unit in the Öceli Tunnel, constructed as part of the Ordu Ring Road Project in northern Türkiye, absorbed water from the surrounding lithological units, causing swelling and the loss of strength. This led to severe deformations and a collapse during tunnel excavation, displacing 160 m³ of material. In addition, Aygar and Gokceoglu (2021) highlighted the significant challenges faced by the Geminbeli Tunnel, located between Zara and Suşehri in Türkiye, in terms of stability at the tunnel portal in a region with high seismicity due to its proximity to the North Anatolian Fault Zone. During construction, failure in the portal area led to deformations and collapses within the tunnel, severely impacting its stability (Aygar, Gokceoglu 2021). The T3 Tunnel, which was built in 1933 with interlocking stone masonry lining, on the Malatya-Narlı Conventional Railway Route was intersected by the surface rupture during the 6 February 2023 Pazarcık Earthquake (Mw 7.7), and a part of the tunnel was damaged completely (Karahan *et al*. 2025).

Hong *et al*. (2021) presented that during excavation of the SV Tunnel on the Dongzhi Plateau in China, water infiltration and reduced soil strength caused unexpected deformations and two sudden collapses in a geological unit known for its high water content and

low strength, called a soft-plastic loess layer. This resulted in structural problems such as block falls, deformations of steel supports, and water accumulation on the tunnel surface (Hong *et al*. 2021).

Yu and Mooney (2023), in their study on the Seattle Northgate Link Extension project, noted that due to a limited number of boreholes, data was limited, particularly at the beginning of the excavation, negatively impacting model performance. They also presented that the predicted ground condition could be completely different during excavation with a TBM. However, Yu, Mooney (2023) also emphasised that the SSL (Semi-supervised learning) model they proposed, given the limited borehole data, provided a more effective measure for determining the ground condition during tunnel construction. Yousuf *et al*. (2025) described the tunnel constructed in the geologically complex and challenging Himalayan region. The tunnel, which was excavated using the New Austrian Tunnelling Method (NATM), was constructed in a young and tectonically active region. The young and tectonically active structure of the region, along with fractured rock masses, shear zones, high local stresses, and frequent seismic activity, caused groundwater intrusion, unexpected collapses, and sudden rockbursts (Yousuf *et al*. 2025).

As studies indicate, problems encountered during tunnel construction due to discrepancies between geological-geotechnical predictions during the investigation phase and actual conditions during the construction phase are common problems worldwide. While studies on minimizing these discrepancies and the presented methodology are widespread in the literature, solid and quantitative studies on these discrepancies are lacking. Therefore, a quantitative approach based on the rock class differences during the investigation and construction phases, the subject of this study, and the quantitative identification of the variables that influence these differences may contribute to addressing a common and significant problem worldwide.

MATERIALS AND METHODS

Tunnels employed

The first stage of any tunnel project is determining the optimum tunnel route. Determining the optimum route includes important parameters such as selecting the most suitable excavation direction, the shortest route, the best slope, diggability, and the best suitability for existing transportation facilities, etc. Project engineers decide on the optimum tunnel route by considering these issues. After the tunnel route is decided, more detailed field investigation studies such as the location of the portals, length of tunnel, and geological conditions are carried out and evaluated in terms of construction cost, construction period, as well as construction and operating conditions. After this stage, detailed field studies are carried out to obtain the engineering geology map of the tunnel route and the geotechnical properties of the rock masses. For this purpose, as many boreholes as possible are performed in the field to enable the modelling of the tunnel body and portals, and geophysical research is carried out. In order to obtain the necessary rock mass parameters, samples of the lithological units on the tunnel route are taken and laboratory studies are carried out. The horizontal and vertical transition of the units with each other along the tunnel route, the effects of discontinuities such as faults, shear zones, contacts, etc., and the effect of water content are the primary effective features in the design of the tunnel. However, high seismicity and in-situ stresses also directly affect the design. The 6 February 2023 earthquake in Türkiye provided important information about the seismic performance of tunnels (Karahan *et al*. 2025; Apostolaki *et al*. 2025). Therefore, the impact of earthquakes and active faults on tunnels requires careful consideration. In the last step of the data collection phase, all the data collected are brought together to create the geological and geotechnical model of the selected tunnel route, and the geological-geotechnical model of the route is created. Using this model, numerical analyses are used to estimate the displacements after tunnel excavation and the necessary supports are determined. Thus, the tunnel project is completed. However, uncertainty plays a critical role in geotechnical design projects (Langford, Diederichs 2015).

In Türkiye, highway tunnels are generally excavated in accordance with the principles of the New Austrian Tunnelling Method (NATM). During the construction phase, the geological condition of the tunnel excavation face is evaluated at each progress step and recorded with face records. This situation enables a comparison between the predicted conditions in the design stage and the actual conditions encountered during tunnel excavation.

In this study, data obtained from the investigation and construction phases of 14 different tunnels were used (Fig. 1). All of the tunnels are double-tube tunnels constructed using NATM.

Yuksekova T-1 Tunnel

The Yuksekova T-1 Tunnel is approximately 4 km long, The T-1 tunnel is located in Hakkari province in the south-east of Türkiye (Fig. 1). Three drillings were performed in the investigation phase of the T-1 tunnel, the lengths of which were 201 m, 212 m, and 100 m. 21 uniaxial compressive strength tests were

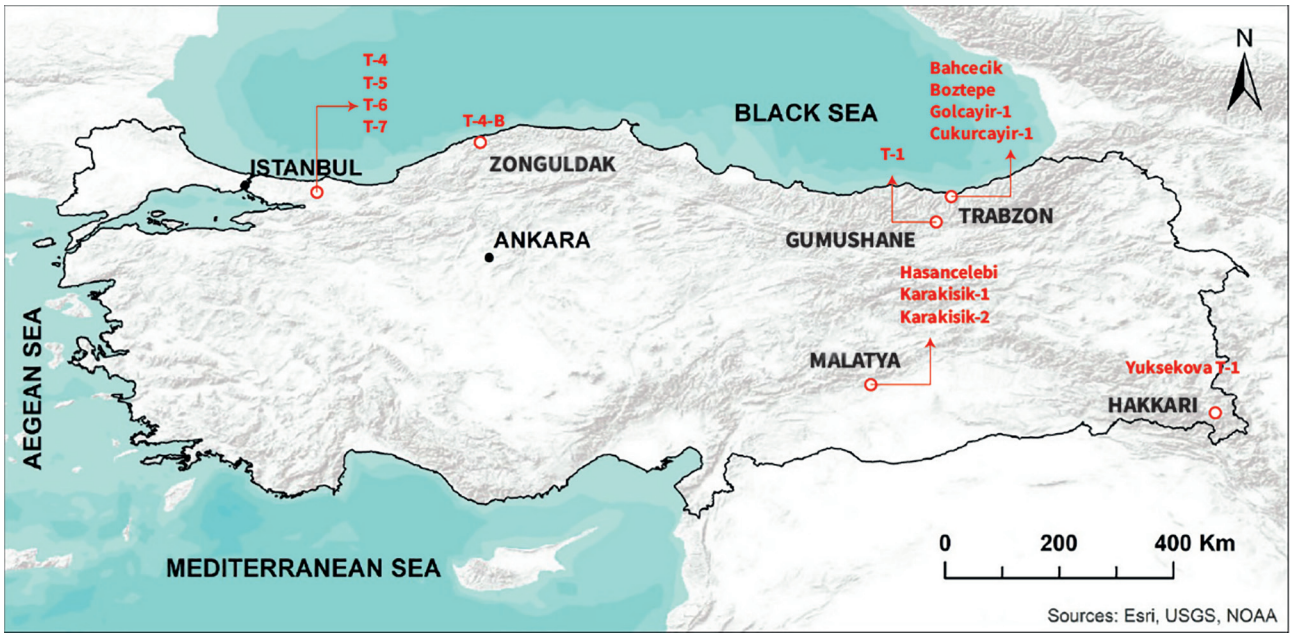

Fig. 1 Location map of the tunnels employed in the study

carried out on the core specimens obtained from these drillings. The Yuksekova Complex consisting of serpentinite, granite and limestone units is seen along the tunnel route, Fig. 2(a). The T-1 tunnel was excavated within the geological units called the Yuksekova Complex. Due to the complex geological properties of Türkiye, several difficulties have been encountered when constructing tunnels in Türkiye (Komu *et al*. 2020; Can *et al*. 2022; Gokceoglu *et al*. 2022).

Boztepe Tunnel

The Boztepe Tunnel, with the left tube 653 m long and right tube 727 m long, is located in Trabzon province in north-eastern Türkiye (Fig. 1). During the investigation phase of Boztepe Tunnel, two drillings were carried out with lengths of 92 m and 118 m. Six uniaxial compressive strength tests were applied on the specimens taken from these drillings. According to the cross-section presented in Fig. 2(b), the Boztepe Tunnel was excavated in brown-grey, slightly-moderately weathered, weak-medium strong basalt units.

Bahcecik Tunnel

The left tube of the Bahcecik Tunnel is 529 m, while its right tube is 540 m long. It is located in Trabzon province in north-eastern Türkiye (Fig. 1). During the investigation phase of the Bahcecik Tunnel, eight drillings were performed with lengths of 115 m, 66 m, 45 m, 45 m, 35 m, 45 m, 50 m, 45 m. A total of 27 uniaxial compressive strength tests were applied on the specimens obtained from these drillings. According to the cross-section presented in Fig. 2(c), the Bahçecik Tunnel was excavated in gray, slightly weathered, moderately strong agglomerate with andesite intrusions in places.

Golcayir Tunnel

The length of the left tube of the Golcayir Tunnel is 444 m, while that of the right tube is 491 m. It is located in Trabzon province in north-eastern Türkiye (Fig. 1). During the investigation phase of the Golcayir Tunnel, a total of 6 drillings with the lengths of 35, 55, 60, 75, 60, and 36 m were performed and a total of 19 uniaxial compressive strength tests were applied on the specimens taken from these drillings. According to the cross-section given in Fig. 2(d), it was excavated within the dark-colored, moderately weathered, weak-medium strength, pyroclastic rocks consisting of volcanic breccia, sandstone, claystone, siltstone, tuff and tuffite alternations belonging to the Kabakoy Formation.

T-4-B Tunnel

The left tube of the T-4-B Tunnel is 1227 m, while its right tube is 1216.5 m long. It is located in Zonguldak province in north-western Türkiye (Fig. 1). In the investigation stage of the T-4-B Tunnel, two drillings with the lengths of 155 and 75 m were performed. A total of 11 uniaxial compressive strength tests were applied on the specimens obtained from the drillings. According to the longitudinal cross-section presented in Fig. 2(e), it was excavated in the volcaniclastic gray, slightly-moderately weathered, medium-strong sandstone, claystone, siltstone alternation belonging to the Gökçetepe Formation.

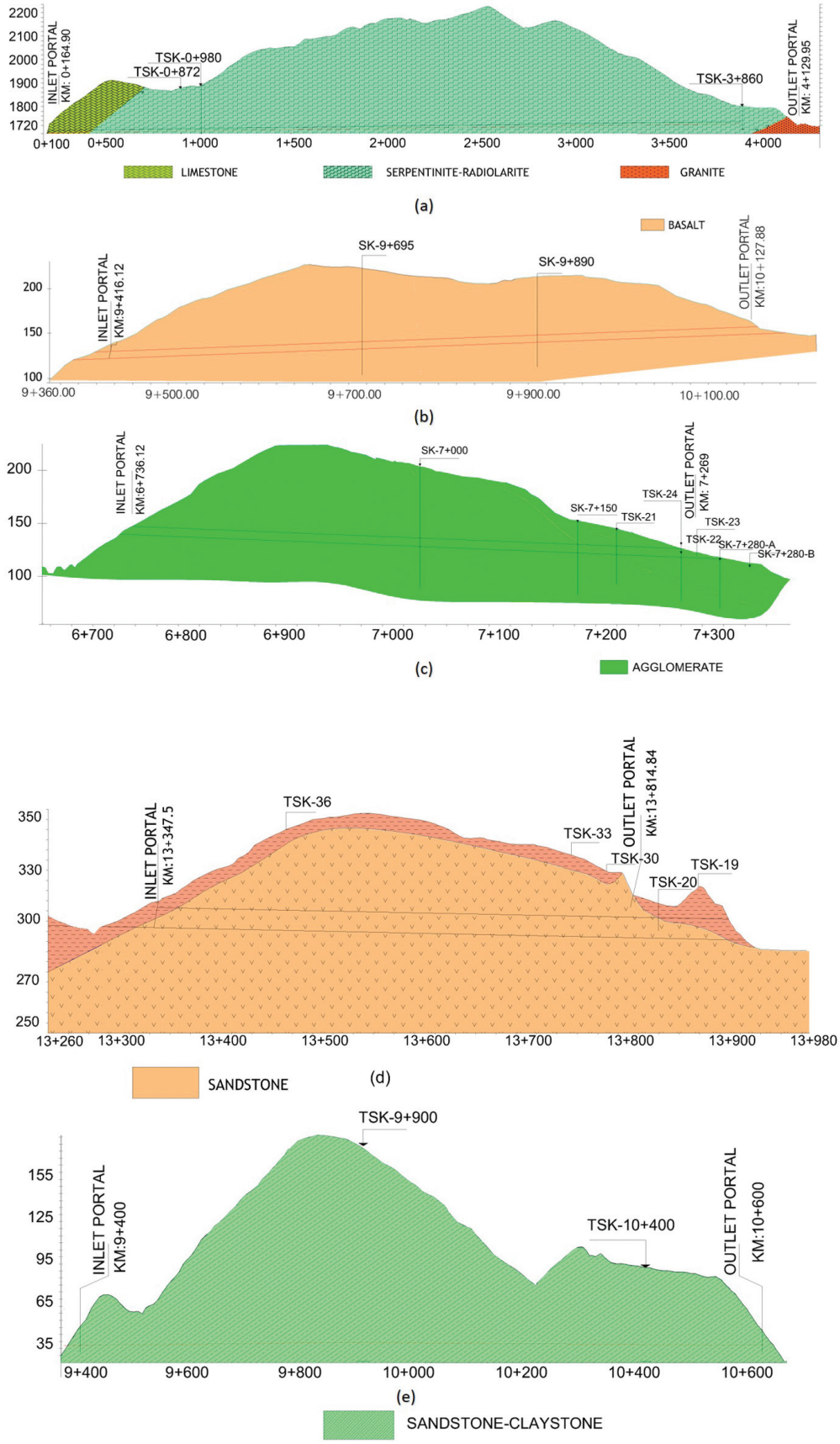

Fig. 2 Longitudinal cross-section of tunnels: Yuksekova T-1 Tunnel (a), Boztepe Tunnel (b), Bahcecik Tunnel (c), Golcayir Tunnel (d), T-4-B Tunnel (e), Cukurcayir-1 Tunnel (f), Gumushane Ring Road T-1 Tunnel (g), Hasancelebi Tunnel (h), Karakisik-1 Tunnel (i), Karakisik-2 Tunnel (j), Sile-Agva T-4 Tunnel (k), Sile-Agva T-5 Tunnel (l), Sile-Agva T-6 Tunnel (m), Sile-Agva T-7 Tunnel (n)

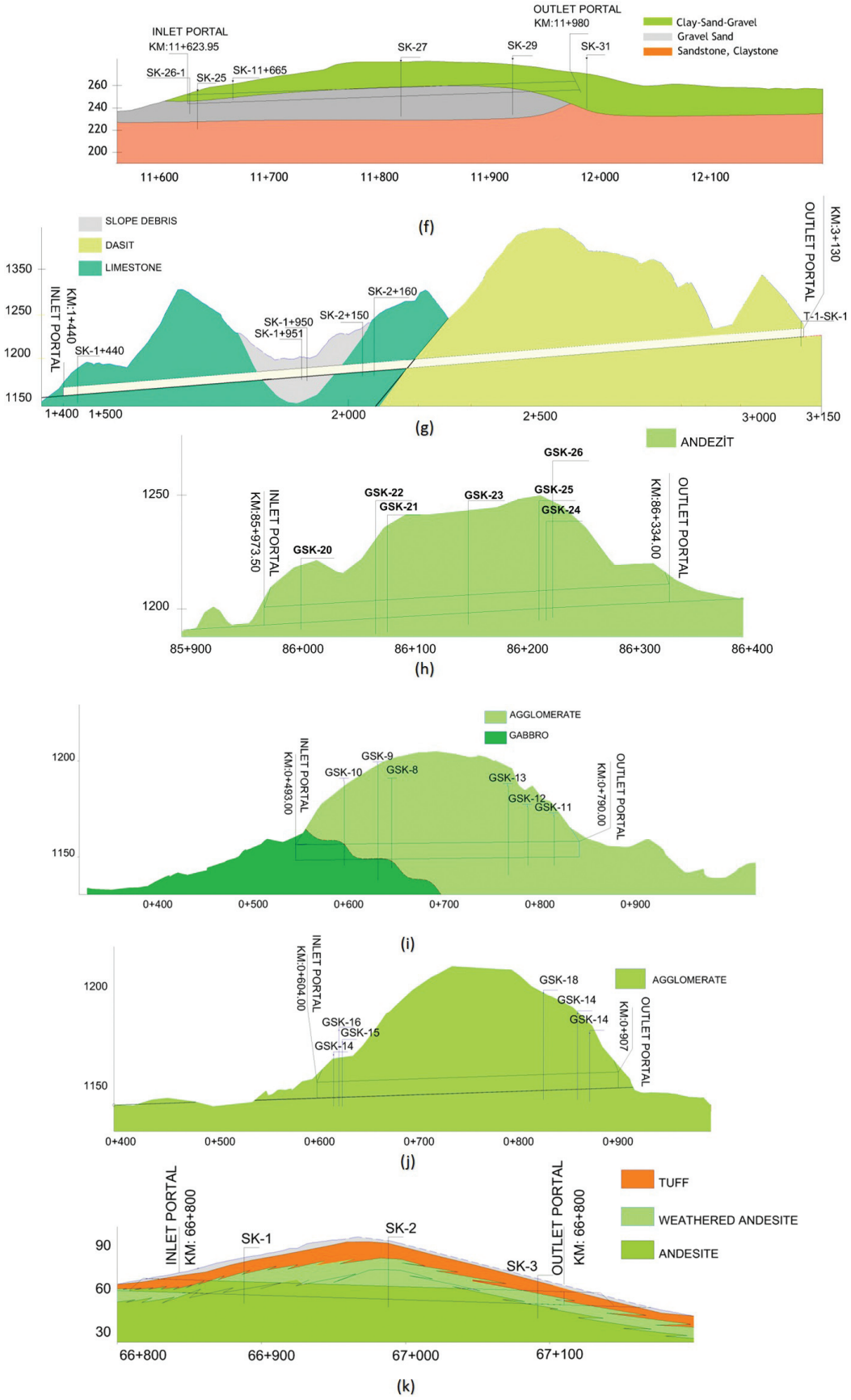

Fig. 2 (continuation) Longitudinal cross-section of tunnels: Yuksekova T-1 Tunnel (a), Boztepe Tunnel (b), Bahcecik Tunnel (c), Golcayir Tunnel (d), T-4-B Tunnel (e), Cukurcayir-1 Tunnel (f), Gumushane Ring Road T-1 Tunnel (g), Hasancelebi Tunnel (h), Karakisik-1 Tunnel (i), Karakisik-2 Tunnel (j), Sile-Agva T-4 Tunnel (k), Sile-Agva T-5 Tunnel (l), Sile-Agva T-6 Tunnel (m), Sile-Agva T-7 Tunnel (n)

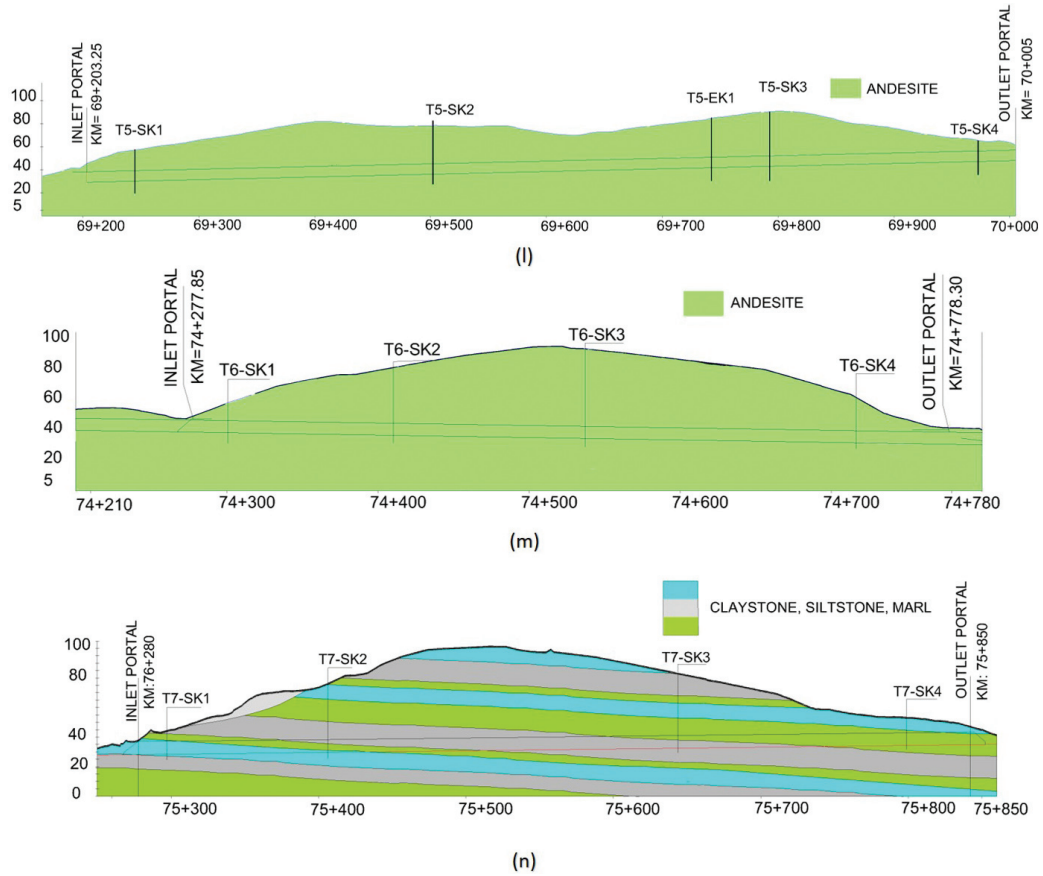

Fig. 2 (continuation) Longitudinal cross-section of tunnels: Yuksekova T-1 Tunnel (a), Boztepe Tunnel (b), Bahcecik Tunnel (c), Golcayir Tunnel (d), T-4-B Tunnel (e), Cukurcayir-1 Tunnel (f), Gumushane Ring Road T-1 Tunnel (g), Hasancelebi Tunnel (h), Karakisik-1 Tunnel (i), Karakisik-2 Tunnel (j), Sile-Agva T-4 Tunnel (k), Sile-Agva T-5 Tunnel (l), Sile-Agva T-6 Tunnel (m), Sile-Agva T-7 Tunnel (n)

Cukurcayir-1 Tunnel

The left tube of the Cukurcayir-1 Tunnel is 378 m long, whereas the right tube is 320 m long. It is located in Trabzon province in north-eastern Türkiye (Fig. 1). During the investigation phase of the Cukurcayir-1 Tunnel, a total of 6 drillings with the lengths of 35, 52, 58, 50, 50 and 45 m were performed and a total of 21 uniaxial compressive strength tests were applied on the specimens taken from these drillings. According to the cross-section given in Fig. 2(f), the excavation was carried out within the yellowish-brown to reddish-brown clay, sandy silty clay, and clay/gravel units of the Kabaköy Formation (Tek) encountered at the surface, which are underlain by an alternation of gravelly clayey sand, very weak strength, weakly cemented sandstone, claystone, and tuff.

Gumushane Ring Road T-1 Tunnel

The length of the left tube of the Gumushane Ring Road T-1 Tunnel is 1710 m, while that of the right tube is 1655 m. It is located in Gumushane province in north-eastern Türkiye (Fig. 1). During the investigation phase of the T-1 Tunnel, a total of 6 drillings with the lengths of 20, 19, 31, 63, 58 and 18 m were performed and a total of 15 uniaxial compressive strength tests were applied on the specimens taken from these drillings. According to the cross-section given in Fig. 2(g), the excavation was carried out within the highly weathered, fragmented, and intensely jointed weak limestones of the Çatak Formation; the gray-brown, medium-strength slope debris consisting of limestone-originated sand, gravel, and blocks; and the greenish-brown, moderately to highly weathered, weak to medium-strength volcanic breccia with weak basaltic cement and dacitic units belonging to the Kızılkaya Formation.

Hasancelebi Tunnel

The length of the left tube of the Hasancelebi Tunnel is 232 m, while that of the right tube is 360 m. It is located in Malatya province in south-eastern Türkiye (Fig. 1). During the investigation phase of the Hasancelebi Tunnel, a total of 7 drillings with the lengths of 34, 48, 52, 47, 30, 55 and 81 m were performed and a total of 56 uniaxial compressive strength tests were applied on the specimens taken from these drillings. According to the cross-section given in Fig. 2(h), it was excavated within the Hasancelebi Volcanics,

generally represented by andesitic and trachytic volcanic rocks with andesitic tuff intercalations, displaying variable colours from light green/blue to brown, porphyritic to glassy textures, and consisting mainly of trachyandesitic lavas and pyroclastic rocks such as agglomerate, breccia, lapilli tuff, and tuff with locally weak to very weak strength near the tunnel portals.

Karakisik-1 Tunnel

The length of the left tube of the Karakisik-1 Tunnel is 297 m, while the right tube length is 288 m. It is located in Malatya province in south-eastern Türkiye (Fig. 1). During the investigation phase of the Karakisik-1 Tunnel, a total of 6 drillings with the lengths of 36, 60, 44, 45, 64 and 46 m were performed and a total of 42 uniaxial compressive strength tests were applied on the specimens taken from these drillings. According to the cross-section given in Fig. 2(i), it was excavated within two main units: the Hocalıkova Ophiolite, represented by predominantly green-coloured ultramafic and mafic rocks such as serpentinized harzburgite, pyroxenite, gabbro, and associated units, and the Hasancelebi Volcanics, composed mainly of trachyandesitic lavas and pyroclastic rocks such as agglomerate, breccia, lapilli tuff, and tuff, generally gray to light green in colour, with variable thickness and locally heterogeneous engineering properties along the tunnel alignment.

Karakisik-2 Tunnel

The length of the left tube of the Karakisik-2 Tunnel is 263 m, while that of the right tube is 302 m. It is located in Malatya province in south-eastern Türkiye (Fig. 1). During the investigation phase of Karakisik-2 Tunnel, a total of 6 drillings with the lengths of 34, 44, 66, 33, 47 and 58 m were performed and a total of 68 uniaxial compressive strength tests were applied on the specimens taken from these drillings. According to the cross-section given in Fig. 2(j), it was excavated within the Hasancelebi Volcanics, generally represented by andesitic and trachytic volcanic rocks with andesitic tuff interlayers, displaying colours from light green/blue to brown and exhibiting porphyritic to glassy textures and consisting mainly of trachyandesitic lavas and pyroclastic rocks such as agglomerate, breccia, lapilli tuff, and tuff, together with locally interbedded andesitic blocks that form the dominant rock mass especially around the portal sections.

Sile-Agva T-4 Tunnel

The Sile-Agva T-4 Tunnel has two tubes and each of these is 267 meters long. It is located in Istanbul province in north-western Türkiye (Fig. 1). During the investigation phase of the Sile-Agva T-4 Tunnel, a total of 3 drillings with lengths of 32, 55, 32 m were performed and a total of 3 uniaxial compressive strength tests were applied on the specimens taken from these drillings. According to the cross-section given in Fig. 2(k), it was excavated within the Riva Formation, mainly composed of andesitic-basaltic andesitic volcanic-derived sand, gravel and block-sized chaotic material including porphyritic agglomerate, andesitic tuff, volcanic breccia and lava, where at the tunnel portals highly weathered, disturbed tuffaceous units overlie very weak–weak, fractured and jointed andesite layers characterized by low rock quality.

Sile-Agva T-5 Tunnel

The length of the left tube of the Sile-Agva T-5Tunnel is 794 m, while that of the right tube is 802 m. It is located in Istanbul province in north-western Türkiye (Fig. 1). During the investigation phase of the Sile-Agva T-5 Tunnel, a total of 5 drillings with the lengths of 27, 55, 60, 60 and 30 m were performed and a total of 2 uniaxial compressive strength tests were applied on the specimens taken from these drillings. According to the cross-section given in Fig. 2(l), it was excavated within the Riva Formation, which consists of chaotic volcanic-derived materials including sand, gravel, and blocks, as well as porphyritic agglomerate, andesitic tuff, volcanic breccia, and lavas; the excavation encountered highly weathered and disturbed tuffaceous units at the surface, underlain by fractured, jointed, and very weak to weak andesite rock units.

Sile-Agva T-6 Tunnel

The length of the left tube of the Sile-Agva T-6Tunnel is 428 m, while that of the right tube is 464 m. It is located in Istanbul province in north-western Türkiye (Fig. 1). During the investigation phase of the Sile-Agva T-6 Tunnel, a total of total 4 drillings with the lengths of 40, 68, 82 and 60 m were performed and a total of 5 uniaxial compressive strength tests were applied on the specimens taken from these drillings. According to the cross-section given in Fig. 2(m), it was excavated within the Riva Formation, consisting of chaotic volcanic-derived sand, gravel, and blocks, including porphyritic agglomerate, andesitic tuff, volcanic breccia, and lavas, where highly weathered tuffaceous units overlie fractured, jointed, and very weak to weak andesite rock units; the excavation also intersected the Çelebi Formation, which is characterized by an alternation of siltstone, clayey limestone, sandstone, and marl.

Sile-Agva T-7 Tunnel

The Sile-Agva T-7 Tunnel has two tubes, both are 540 meters long. It is located in Istanbul province in

north-western Türkiye (Fig. 1). During the investigation phase of the Sile-Agva T-7 Tunnel, a total of 4 drillings with the lengths of 40, 75, 70 and 40 m were performed and a total of 16 uniaxial compressive strength tests were applied on the specimens taken from these drillings. According to the cross-section given in Fig. 2(n), it was excavated within the Celebi Formation, consisting predominantly of interbedded fractured siltstone and claystone with marl interlayers, locally including dirty white micritic limestones and marls with sandy and silty lenses, representing a lacustrine depositional environment.

STATISTICAL ANALYSES

Statistical analyses play a crucial role in assessing the impact of geological and geotechnical uncertainties encountered during tunnel design and construction and in minimizing these uncertainties. The statistical analyses conducted in this study quantitatively demonstrate the differences between data obtained during the investigation phase and the actual conditions encountered during excavation, allowing us to identify the parameters that influence these uncertainties. Consequently, the statistical analyses performed within the scope of this study were conducted by evaluating the differences between the predictions obtained from the studies performed during the investigation phase of fourteen different tunnels and the actual rock conditions encountered during the construction phase.

Table 1 shows the names and lengths of the drillings performed in 14 tunnels considered in the study, the number of uniaxial compressive strength (UCS) tests performed on the core samples taken from the drillings, and the arithmetic average of the RQD and TCR values obtained from the drillings. While explicit structural geology metrics such as fault density or anisotropy indices were not independently measured, their influence is implicitly integrated into the RQD and TCR values. In rock mechanics, RQD is a direct function of discontinuity frequency and orientation, effectively serving as a proxy for the structural integrity of the rock mass. Similarly, TCR reflects the overall recovery quality, which is heavily influenced by lithological transitions and shear zones. By utilizing these standardized characteristics parameters, the study ensures that the predictive models remain applicable to conventional tunnel projects where specialized structural entropy metrics may not be available, while still accounting for the cumulative effect of geological complexities on prediction uncertainty. Table 2 shows the values of the dependent and independent variables used in the statistical analyses. It should be noted that the RQDn and TCRn variables are the proportional expression of the average RQD and TCR values per tunnel unit length. Accordingly, LDn is the ratio of the total length of the boreholes to the tunnel length, while TCRn, RQDn, and UCSn represent the spatial frequency of data acquisition. This normalization was implemented to establish a standardized metric for Investigation Information Density (IID), ensuring that the predictors reflect the sampling frequency relative to the project scale rather than absolute quantities.

Accordingly:

- LDn is the ratio of the total length of the boreholes along the tunnel line to the tunnel length. Therefore, LDn is the ratio of the borehole length per unit tunnel length.
- TCRn is the ratio of the arithmetic mean of the total core yield (TCR) values obtained from boreholes drilled along the tunnel to the tunnel length.
- RQDn is the ratio of the arithmetic mean of the rock quality designation (RQD) values obtained from boreholes drilled along the tunnel to the tunnel length.
- UCSn is the ratio of the number of uniaxial compressive strength tests performed on core samples obtained from boreholes drilled along the tunnel to the tunnel length.

It is important to distinguish between the physical rock mass properties (RQD, TCR) and the normalized indices (RQDn, TCRn) used in this predictive framework. While RQD is a dimensionless percentage representing rock quality, RQDn can be defined as a Spatial Representativeness Index. The division by tunnel length (L) serves to weight the observed rock quality by the investigation's spatial extent. Physically, this can be interpreted as the integrated quality-information density along the tunnel axis. This normalization is necessary to prevent 'information inflation' in longer tunnels and to ensure that the

Table 1 The resulting bootstrap-based uncertainty bounds for MPAD summary statistics

Metric	Estimate	95% Bootstrap CI
Mean MPAD (%)	16.82	[10.34, 23.77]
Median MPAD (%)	9.00	[5.14, 15.62]
Proportion of sections with MPAD < 10%	0.536	[0.357, 0.750]
Standard deviation of MPAD (%)	19.03	–
IQR (Q1–Q3) of MPAD (%)	15.68 (3.51–19.19)	–
Min–Max MPAD (%)	0.17–73.05	–

Table 2 Data obtained in the tunnels

Name of Tunnel		LDn* (ratio)	TCRn* (ratio)	RQDn* (ratio)	UCSn* (ratio)	MPAD* (%)
Yuksekova T-1	Left tube	0.13	1.92	0.94	0.005	73.05
	Right tube	0.13	1.93	0.94	0.005	38.95
Bahcecik	Left tube	0.58	16.62	9.40	0.025	17.74
	Right tube	0.26	16.23	9.09	0.026	15.62
Boztepe	Left tube	0.14	15.14	10.44	0.005	6.47
	Right tube	0.16	13.54	12.34	0.004	6.68
T-4-B	Left tube	0.19	6.76	5.60	0.009	9.48
	Right tube	0.19	6.82	5.65	0.009	8.23
Golcayir-1	Left tube	0.60	17.79	10.90	0.034	2.31
	Right tube	0.46	17.31	10.97	0.032	0.17
Cukurcayir-1	Left tube	0.54	7.53	2.03	0.05	15.38
	Right tube	0.27	9.14	2.58	0.01	15.38
GCY T-1	Left tube	0.07	4.00	1.00	0.004	45.95
	Right tube	0.09	4.00	2.00	0.005	46.69
Hasancelebi	Left tube	0.91	40.10	72.00	0.160	5.03
	Right tube	0.78	26.27	54.00	0.121	1.74
Karakisik-1	Left tube	0.48	34.60	15.00	0.08	8.52
	Right tube	0.52	28.88	13.00	0.07	10.24
Karakisik-2	Left tube	0.31	37.26	20.00	0.11	5.25
	Right tube	0.54	33.05	20.00	0.13	3.81
SA-T-4	Left tube	0.45	31.00	7.00	0.011	23.53
	Right tube	0.45	31.00	7.00	0.011	15.69
SA-T-5	Left tube	0.29	9.70	1.10	0.003	1.63
	Right tube	0.29	9.60	1.10	0.003	1.63
SA-T-6	Left tube	0.42	17.00	10.00	0.030	0.85
	Right tube	0.42	17.00	10.00	0.030	2.61
SA-T-7	Left tube	0.59	21.24	2.98	0.012	56.77
	Right tube	0.54	19.59	2.75	0.011	31.51

*LDn: The ratio of drilling length to tunnel length, TCRn: The ratio of the arithmetic mean of the TCR (total core recovery) values to tunnel length, RQDn: The ratio of the arithmetic mean of the RQD (rock quality designation) values to tunnel length, UCSn: The ratio of the arithmetic mean of the number of UCS (uniaxial compressive strength) test to tunnel length, MPAD: Mean percent absolute difference.

statistical model evaluates the reliability of the investigation phase based on how comprehensively the rock mass was characterized relative to the total excavation volume. The normalization of investigation parameters (LDn, TCRn, RQDn, and UCSn) by tunnel length was implemented to establish a standardized metric for Investigation Information Density (IID). In geotechnical practice, the reliability of a geological model is directly proportional to the sampling frequency relative to the project dimensions. Since the tunnels in this study vary significantly in length, using absolute values would introduce a scale-dependent bias. Normalization ensures that the predictors reflect the spatial frequency of data acquisition, allowing the statistical models to evaluate the impact of investigation intensity on MPAD across different project scales. This approach treats each tunnel unit length as a standardized sampling domain consistent with the principles of Representative Sample Volume (RSV) and statistical sampling theory in rock mechanics.

The mean absolute percentage difference (MPAD),

Table 3 MPAD sample calculation for Yuksekova T-1 Tunnel

No	RMR		Difference, %
	Investigation	Construction	
1	37	39	5.13
2	37	39	5.13
3	45	39	–15.4
4	45	42	–7.14
5	45	42	–7.14
6	45	42	–7.14
7	45	42	–7.14
191	41	39	–5.13
192	41	39	–5.13
193	41	39	–5.13
194	41	15	–173.33
195	41	15	–173.33
196	48	15	–220
197	48	15	–220
198	45	15	–200
199	45	39	–15.39
Mean Percent Absolute Difference, MPAD, %			73.05

used as the dependent variable in statistical analyses, is the absolute arithmetic mean of the percentage change between the estimated RMR (rock mass rating) scores during the investigation phase and the calculated RMR score differences encountered at the tunnel face during the construction phase. For each tunnel, the RMR values, calculated based on the geological conditions encountered at the tunnel face during the construction phase and predicted during the investigation phase, were calculated at 20-meter intervals. For example, for the Yuksekova T-1 Tunnel, when the RMR values from the investigation and construction phases were compared at 20-meter intervals, approximately 200 absolute percentage difference values were obtained for each tunnel tube. The arithmetic average of these values was then calculated for the right and left tubes of each tunnel (Table 3). This calculation was also performed at 20-meter intervals for the other tunnels. This 20-meter interval was specifically selected to balance the resolution of excavation face mapping with the spatial frequency of investigation boreholes, thereby ensuring statistical stability while filtering out localized geological noise that could otherwise distort the MPAD calculations. Therefore, a precise difference analysis was performed for each tunnel, increasing the number and precision of data.

To account for the inherent variability in rock mass conditions and to provide a measure of statistical reliability, 95% Confidence Intervals (CI) were calculated for the MPAD values using a non-parametric Bootstrap resampling procedure (1.000 iterations). This uncertainty quantification ensures that the reported discrepancies are not merely point estimates but reflect the range of variability encountered along the tunnel route. By providing confidence bounds, the study allows for a more nuanced comparison between tunnels, where overlapping intervals indicate statistically similar investigation-phase performance, while non-overlapping intervals highlight significant differences in prediction accuracy. The resulting bootstrap-based uncertainty bounds for MPAD summary statistics are reported in Table 1.

The primary objective of the statistical analysis was to determine whether the discrepancy between investigation phase predictions and excavation phase determinations (MPAD) can be systematically explained by investigation intensity and rock mass quality indicators, or whether such discrepancies occur randomly. To address this, a structured multi-stage statistical framework was implemented, progressing from diagnostic testing to parsimonious modelling, regularization, non-linear ensemble learning, and significance validation.

Model selection was conducted using a multi-criteria approach to ensure both statistical parsimony and predictive reliability. For linear and regularized regression models (OLS and Elastic Net), Akaike Information Criterion (AIC) and Bayesian Information Criterion (BIC) were utilized to identify the optimal balance between model fit and complexity, effectively penalizing the inclusion of non-significant predictors. For the ensemble-based Random Forest model, predictive performance was assessed using Nested Cross-Validation, focusing on Root Mean Square Error (RMSE) and Mean Absolute Error (MAE) as primary indicators of generalization capability. This comprehensive evaluation framework ensures that the selected models are not merely optimized for the training data (R^2) but are robust tools for predicting MPAD in independent tunnel projects.

It should be emphasized that the comparison of multiple functional forms (linear, regularized linear, and ensemble-based models) does not represent parallel hypothesis testing. Instead, it constitutes a predictive model selection process. Linear models were evaluated using information-theoretic criteria (AIC and BIC), which penalize excessive complexity, while non-linear models were assessed using Nested Cross-Validation to obtain unbiased generalization error estimates. These procedures mitigate the risk of overfitting and reduce the likelihood of spurious model superiority arising from multiple comparisons.

Residual diagnostics were conducted for the OLS models to assess compliance with classical regression assumptions. Residual-versus-fitted plots did not indicate systematic heteroscedastic patterns. The Breusch–Pagan test yielded non-significant results ($p > 0.05$), suggesting homoscedastic variance. The Shapiro-Wilk test indicated mild deviations from strict normality, which is common in small-sample geotechnical datasets. Given that the primary focus of this study is predictive performance rather than parameter inference and considering that regularized and ensemble-based models were also employed, minor deviations from normality are not expected to materially affect the study conclusions.

Prior to model development, multicollinearity among the independent variables was assessed using the Variance Inflation Factor (VIF). All predictors yielded VIF values below 5.0 (LDn = 2.36, TCRn = 2.64, RQDn = 3.65, UCSn = 4.59), indicating the absence of severe multicollinearity. Nevertheless, the relatively high pairwise correlation between RQDn and UCSn (r = 0.839) was noted. To mitigate the potential influence of this correlation on coefficient stability, Elastic Net regularization was employed as the primary predictive model, as it simultaneously performs variable selection and coefficient shrinkage, providing robust estimates under moderate multicollinearity conditions.

In this study, geological heterogeneity is reflected

by the spatial variance of the RMR scores encountered during the excavation phase. Tunnels characterized by high MPAD values typically exhibited frequent and high-magnitude fluctuations in rock mass classes at 20-meter intervals, indicating complex structural conditions and lithological variations. This spatial variations in rock mass quality represents the inherent heterogeneity that challenges investigation-phase predictions. By analyzing the discrepancy (MPAD) across these high-variance sections, the study implicitly accounts for geological complexity, as higher variance in encountered RMR scores directly correlates with increased prediction uncertainty.

It should be noted that the tunnels included in this study encompass a variety of geological settings and lithological units. The proposed statistical framework does not assume that these tunnels are geologically comparable in terms of their absolute rock mass properties. Instead, it focuses on the comparability of investigation-phase performance. By utilizing normalized indices (LDn, TCRn, RQDn, and UCSn), the study evaluates how the intensity and quality of data acquisition influence the reliability of RMR predictions across diverse geological environments. This approach treats the investigation process as a standardized engineering activity, where the goal is to minimize the discrepancy (MPAD) between predicted and encountered conditions, regardless of the inherent lithological differences. This generalization is essential for developing a broadly applicable uncertainty quantification tool for tunnel projects.

Within the scope of this study, a multi-layered statistical evaluation framework was implemented to ensure the reliability and scientific validity of the findings derived from the dataset (n = 28). Initially, data diagnostics were performed using Pearson correlation matrices and Variance Inflation Factor (VIF) analysis to detect potential multicollinearity issues among the geological predictors (LDn, TCRn, RQDn, and UCSn). Given the constraints of the sample size and the inherent correlations between rock mass parameters, the regularized regression via the Elastic Net algorithm was employed to prevent overfitting through simultaneous L1 and L2 penalization. To identify the most parsimonious and interpretable model, an exhaustive "Best Subset Selection" was conducted based on the Akaike Information Criterion (AIC) and Bayesian Information Criterion (BIC). Furthermore, to capture potential non-linear relationships, a Random Forest (RF) machine learning model was developed. To mitigate bias in performance estimation for the small dataset, the RF model was validated using a Nested Cross-Validation (Nested-CV) approach and Leave-One-Out Cross-Validation (LOOCV). Finally, the engineering relevance of the proposed Mean Percent Absolute Difference (MPAD) metric was evaluated to justify its application in tunnel investigation and excavation phases.

Data diagnostics and multicollinearity analysis

Before constructing multi-input models, diagnostic analyses were conducted to evaluate the statistical behaviour of the independent variables. Pearson correlation coefficients were calculated to assess pairwise linear relationships among LDn, TCRn, RQDn, and UCSn. In addition, Variance Inflation Factor (VIF) analysis was performed to quantify the degree of multicollinearity.

The purpose of this step was to determine whether interdependencies among investigation parameters could destabilize regression coefficients, particularly given the limited sample size (n = 28). The correlation matrix indicated a relatively high correlation between RQDn and UCSn (r = 0.84). However, VIF values remained below the commonly accepted critical threshold of 5 (LDn = 2.36; TCRn = 2.64; RQDn = 3.65; UCSn = 4.59), indicating that severe multicollinearity was not present (Fig. 3). Although the predictors were statistically admissible, the observed inter-correlations justified the subsequent use of regularized regression techniques to enhance model robustness.

Regularized regression: Elastic Net

Considering the moderate inter-correlations among predictors and a relatively small dataset, Elastic Net regression was employed. Elastic Net combines L1 (Lasso) and L2 (Ridge) regularization, penalizing large coefficients and reducing overfitting while maintaining predictive stability (Table 4).

Hyperparameters (α and L1_ratio) were optimized using Leave-One-Out Cross-Validation (LOOCV), which is particularly suitable for small datasets as it maximizes training data usage in each iteration.
The optimal model parameters were determined as:

$$\alpha = 1.84$$

$$L1\_ratio = 0.10$$

The low l1_ratio indicates that the model behaviour was closer to Ridge regression, suggesting that coefficient shrinkage rather than variable elimination was more appropriate for this dataset.

All standardized coefficients exhibited negative signs, indicating that increasing investigation intensity per unit tunnel length reduces MPAD. Among the predictors, TCRn showed the strongest influence (−1.70), followed by UCSn (−1.42), RQDn (−1.41), and LDn (−1.10).

Observed versus predicted MPAD values for the Elastic Net model (n = 28) are given in Fig. 4. Although the explanatory power is moderate, the model demonstrates consistent directional behavior and im-

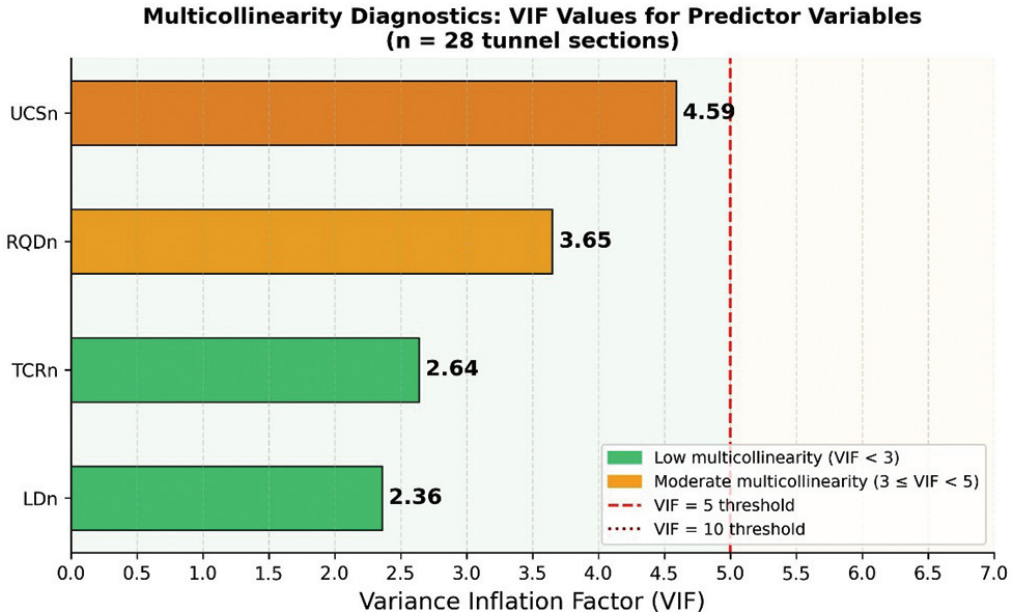

Fig. 3 Multicollinearity diagnostics for the investigation indicators (n = 28). The Variance Inflation Factor (VIF) values for all predictors remain below the moderate threshold of 5, indicating that the model coefficients are statistically stable and not severely distorted by inter-variable correlations

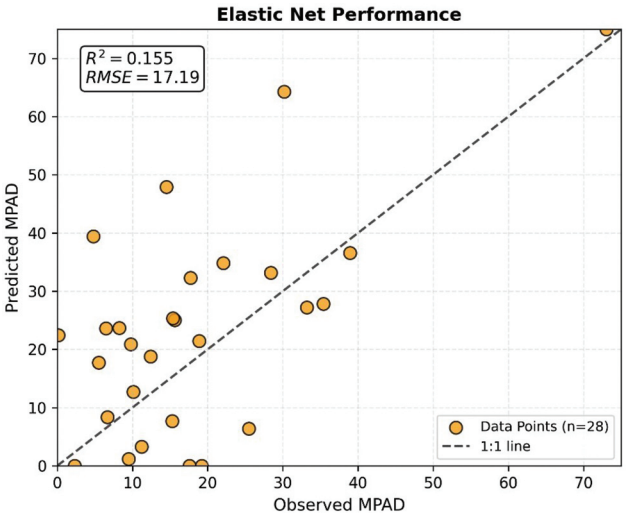

Fig. 4 Observed versus predicted MPAD values for the Elastic Net model (n = 28)

Table 4 Performance and parameters of the Elastic Net model

Parameter/ Metric	Value
Optimal Alpha (Penalty Strength)	1.84
Optimal L1 Ratio (Mixing)	0.10 (Ridge-dominant)
RMSE (Root Mean Squared Error)	17.19
MAE (Mean Absolute Error)	13.00
R^2 (Overall Fit)	0.155

Table 5 Comparison of candidate OLS models based on information criteria

Model Structure	AIC	BIC	ΔAIC	Status
MPAD ≈ TCRn	242.64	245.31	0.00	Best Model
MPAD ≈ RQDn	243.12	245.78	0.48	Competitive
MPAD ≈ TCRn + LDn	244.41	248.41	1.77	Less Efficient
Full Model (All 4)	247.77	254.43	5.13	Over-parameterized

ΔAIC > 2 indicates significantly less support for the model compared to the best model.

proved stability compared to ordinary least squares under correlated predictors (Fig. 4).

Parsimonious model selection using information criteria (AIC/BIC)

To address concerns related to over-parameterization in small datasets, an exhaustive Best Subset Selection procedure was conducted. Model combinations were compared using Akaike Information Criterion (AIC) and Bayesian Information Criterion (BIC), which penalize model complexity while rewarding explanatory power. This analysis was performed to identify the most parsimonious model that adequately explains MPAD without unnecessary predictors.

The results showed that the single-variable model including only TCRn produced the lowest AIC (242.64) and BIC values, outperforming multi-variable alternatives. The regression coefficient for TCRn was statistically significant ($p \approx 0.04$), indicating that TCRn alone provides the most efficient explanation of MPAD variability within the dataset (Table 5). The predictive performance and the alignment of this parsimonious OLS model with the observed data are illustrated in Fig. 5. The full four-variable model showed higher AIC and BIC values, confirming that additional predictors do not improve model efficiency under the current sample size. This finding highlights

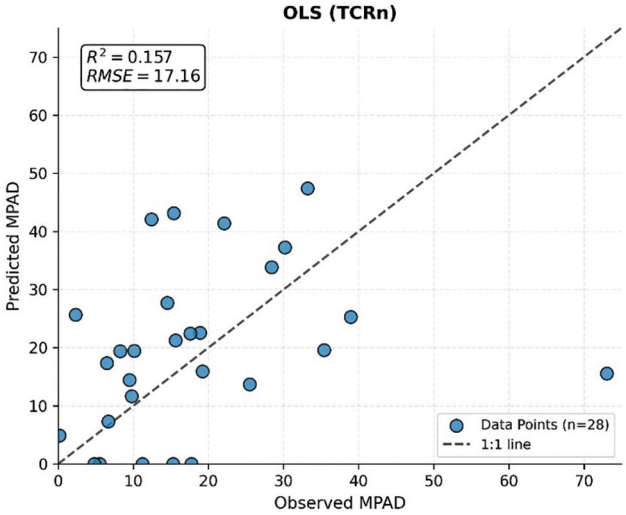

Fig. 5 Performance of the parsimonious OLS model using TCRn as the sole predictor (n = 28)

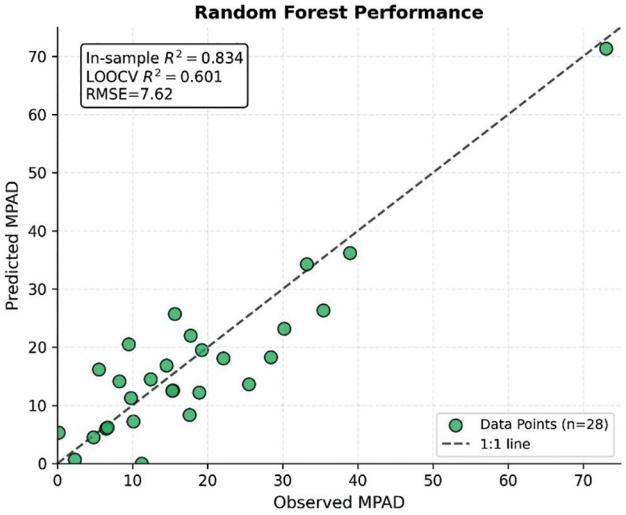

Fig. 6 Performance of the Random Forest model (n = 28)

TCRn as the most influential and statistically robust investigation parameter in explaining discrepancies between investigation and construction phases.

Non-linear modelling via Random Forest and Nested Cross-Validation

Given the limited generalization performance of linear and regularized models, a non-linear ensemble approach was considered necessary to capture potential interaction effects and threshold-like behaviours among geological predictors. To capture potential non-linear interactions between geological parameters and MPAD, a Random Forest (RF) regressor was employed. To ensure methodological validity for the expanded dataset (n = 28) and prevent overfitting, a Nested Cross-Validation (Nested CV) framework was implemented (Fig. 6). This approach consists of an inner loop (3-fold CV) for hyperparameter tuning (e.g., tree depth, number of estimators) via Grid Search, and an outer loop (5-fold CV) for unbiased performance estimation on unseen data. Additionally, the Out-of-Bag (OOB) score was reported as an internal validation mechanism, providing a robust estimate of the model's generalization capability without the need for a separate test set.

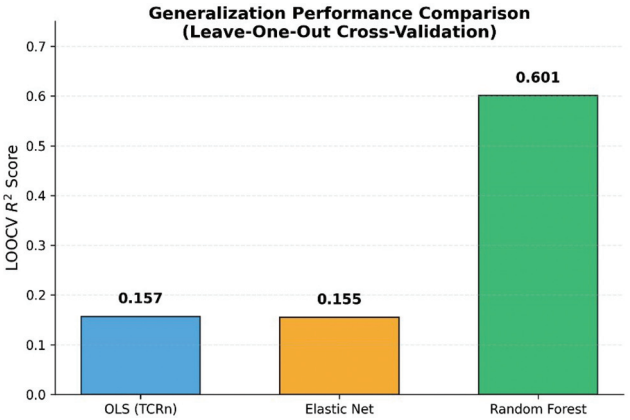

Fig. 7 Comparison of generalization performance across models using Leave-One-Out Cross-Validation (LOOCV) R^2 scores. The Random Forest model significantly outperforms linear baselines (OLS and Elastic Net), capturing approximately 60% of the variance in investigation-excavation discrepancies, whereas linear models are limited to approximately 15%

The Random Forest model demonstrated superior predictive performance compared to linear models, achieving a LOOCV $R^2$of 0.60 and an OOB score of 0.55 (Fig. 6). The consistency between the internal (OOB) and external (LOOCV) validation scores confirms that the model has successfully captured a stable signal rather than overfitting to the training data as can be seen from Fig. 7. These results indicate that the relationship between rock mass quality and investigation-excavation discrepancy is inherently non-linear, requiring ensemble-based modelling to achieve high predictive accuracy.

Feature importance analysis and predictor hierarchy

To identify the relative contribution of each geological and investigation-related parameter to the prediction of MPAD, a Feature Importance analysis was conducted based on the Random Forest model. This analysis utilizes the 'Gini Importance' or 'Mean Decrease in Impurity' to rank the predictors. By quantifying the importance of each feature, we can determine which aspects of the tunnel investigation phase (e.g., drilling density vs. core quality) have the most significant impact on reducing the discrepancy between predicted and encountered rock mass conditions.

The feature importance analysis revealed that RQDn (≈ 31%), TCRn (≈ 30%), and LDn (≈ 29%) contribute almost equally to MPAD prediction, while UCSn (≈ 10%) plays a comparatively minor role (Fig. 8). These results suggest that for the investigated tunnels, the overall quality of the drilling process and the spatial coverage of the investigation are more decisive in accurate rock mass classification than individual laboratory strength tests.

Statistical significance via permutation testing

Permutation testing was conducted after final model decision to ensure that the reported cross-validated performance was not the result of optimistic bias introduced during hyperparameter tuning. In this procedure, the target labels (MPAD values) were randomly shuffled while keeping the predictor variables (LDn, TCRn, RQDn, UCSn) constant, and the model was retrained in each iteration. This process generates a null distribution of performance metrics (e.g., R^2) that would be expected by chance alone. The empirical *p*-value was then calculated by comparing the original model's performance against this null distribution. A low *p*-value indicates that the observed predictive power is highly unlikely to have occurred by random chance.

The permutation test yielded a significant *p*-value of 0.002 (Table 6), demonstrating that the Random Forest model's predictive performance is not an artifact of random association or overfitting. While the models trained on shuffled data failed to show any predictive power (mean $R^2 = -0.44$), the original model consistently and significantly outperformed the null distribution (Fig. 9). This result provides strong statistical evidence that the identified relationships between investigation-phase parameters (LDn, TCRn, RQDn, UCSn) and MPAD are unique and reflect a representative underlying signal in the geotechnical dataset, confirming the model's ability to generalize beyond the training samples even within a specialized engineering context.

The LOOCV-based error comparison is given in Fig. 10. The Random Forest model substantially reduces both RMSE and MAE relative to the linear baselines, confirming that the gain observed in LOOCV R^2 is also reflected in lower absolute prediction errors. Under LOOCV, the Random Forest model achieves an RMSE of 11.28 and an MAE of 7.49, whereas OLS (TCRn) and Elastic Net yield higher

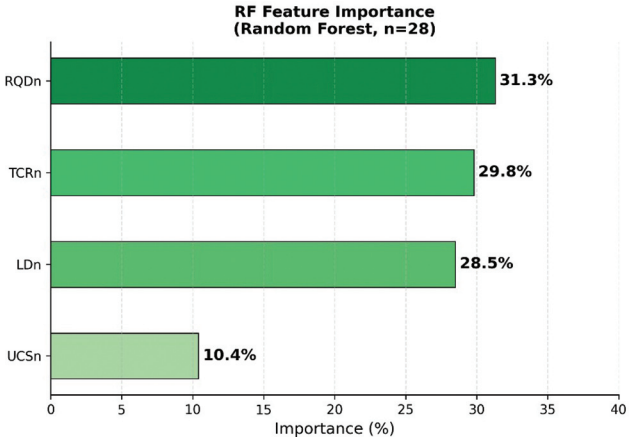

Fig. 8 Relative importance of investigation indicators derived from the validated Random Forest model (n = 28). RQDn, TCRn, and LDn collectively account for approximately 90% of the predictive contribution, while UCSn plays a comparatively minor role in explaining investigation-excavation discrepancies

Table 6 Statistical significance results from the Permutation Test (n = 28; 500 iterations)

Metric	Original Model Value	Permutation Mean (Chance)	*p*- value
R^2 Score	0.64	-0.44	0.002
RMSE	11.28	22.32	0.002

*$p < 0.01$ indicates that the model`s performance is statistically significant.

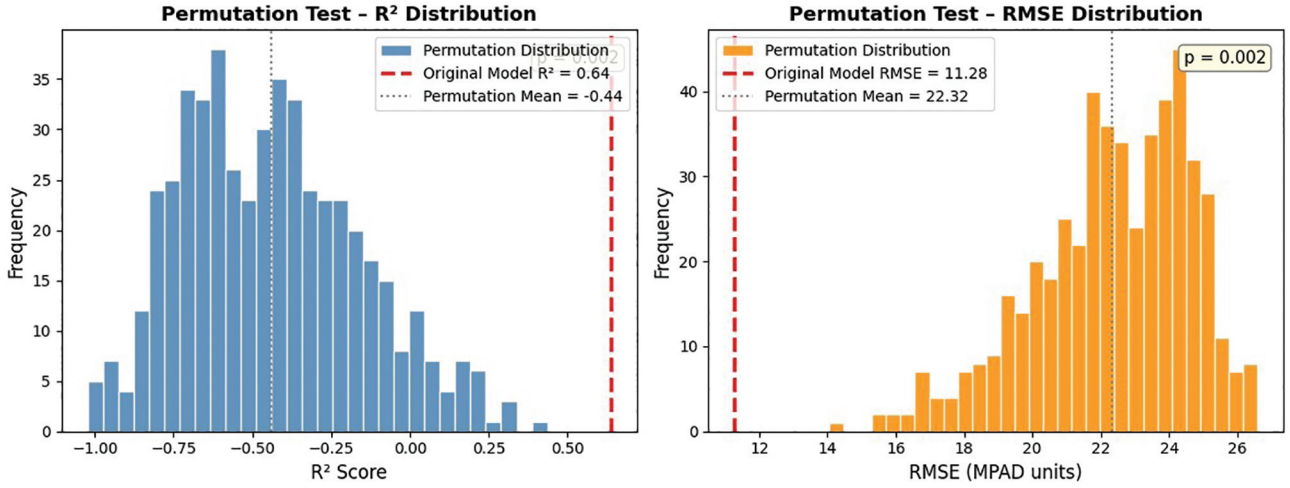

Fig. 9 R^2 and RMSE distributions of permutation test

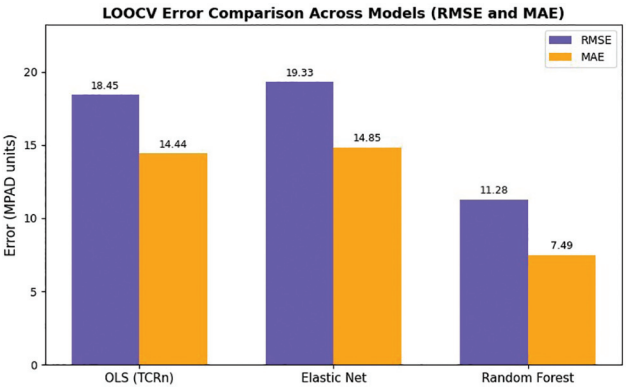

Fig. 10 Comparison of prediction errors across models under Leave-One-Out Cross-Validation (LOOCV)

error levels (RMSE ≈ 18.5–19.3, MAE ≈ 14.4–14.9). This pattern indicates clearly improved generalization performance for the Random Forest model compared to the linear alternatives.

Engineering interpretation and interaction analysis via 2D-PDP

While the previous sections establish the statistical validity and significance of the Random Forest model, this section explores the practical engineering implications of the identified relationships. To visualize how the investigation-phase indicators (TCRn, RQDn, and LDn) interact to influence the prediction-excavation discrepancy (MPAD), two-dimensional Partial Dependence Plots (2D-PDP) were produced (Fig. 11). These plots provide a 'geotechnical decision map' for investigation planning by illustrating the predicted MPAD levels across varying combinations of predictors and highlighting the 10% precision threshold. It should be emphasized that partial dependence plots describe model-based marginal effects rather than direct causal relationships. Nevertheless, they provide a consistent and interpretable approximation of how MPAD responds to simultaneous variations in investigation parameters, offering a quantitative basis for optimizing site investigation intensity within the observed data range.

The interaction between core recovery quality (TCRn) and rock mass quality (RQDn) is illustrated in Fig. 11 (left). The white dashed contour line represents the target MPAD level of 10%, which serves as a critical precision threshold for geotechnical data need for a reliable tunnel design. The analysis reveals a pronounced non-linear sensitivity: in poorer rock masses (lower RQDn), the model is highly sensitive to core recovery, requiring a significantly higher TCRn (typically > 15.0) to maintain the 10% discrepancy level. Conversely, in more competent rock masses, the requirement for TCRn is slightly relaxed, although high core recovery remains a primary driver for minimizing predictive uncertainty. The 2D-PDP analysis (Fig. 11, right) identifies a clear performance plateau for the predictive model regarding investigation intensity. A critical threshold of 10% MPAD is established as a benchmark for robust geotechnical characterization. To maintain this precision level, the interaction between core recovery and drilling density suggests that a TCRn > 12.5 combined with an LDn > 0.35 is required. These surfaces confirm that geological uncertainty is not a function of a single parameter but emerges from the interplay between the inherent rock mass complexity and the quality of the investigation process. By utilizing these interaction maps (Fig. 11), tunnel engineers can quantitatively determine the necessary investigation intensity and data quality required to stay within acceptable discrepancy limits for specific geological settings. This transformation of MPAD from a descriptive metric into a prescriptive design tool allows for more objective decision-making in site investigation planning.

DISCUSSION

The core outcome of this study is that the discrepancy between investigation-phase predictions and excavation-phase observations, expressed by MPAD, is systematically related to the Investigation Information Density (IID) indicators (LDn, TCRn, RQDn, UCSn). The results support the risk-based view of rock engineering as decision-making under uncertainty (Spross *et al*. 2020) and the growing emphasis on safety/risk in underground projects (Benardos, Kaliampakos 2017). Within the dataset constructed in the study, increasing investigation intensity and quality are associated with lower MPAD, i.e., more reliable anticipation of excavation conditions. This aligns with the argument that a geological model is "reliable" only if it helps foresee rock mass behaviour and prevents unpleasant surprises during excavation (Perello 2011). Importantly, the study also responds to a practical gap noted for Eurocode 7 applications: although reliability-based and observational methods are recommended, explicit guidance on which parameters should be observed is not provided (Bjureland *et al*. 2017).

MPAD is a continuous, transparent metric that summarizes investigation–construction mismatch; however, its engineering meaning is context-dependent because not every RMR deviation leads to the same consequence. In practice, mismatches that push conditions across rock mass class boundaries can force immediate revisions in excavation sequence and support classes–exactly the kind of mechanism that contributes to cost and schedule overruns frequently observed in tunneling projects (Isaksson, Stille 2005). The manuscript's broader context and case literature

emphasize how prediction errors and incomplete geological interpretation can translate into severe construction problems (e.g., Merrie 2009; Li *et al*. 2010; Thum, De Paoli 2015; Huang *et al*. 2016; Liu *et al*. 2020; Yum *et al*. 2020; Hong *et al*. 2021). In Türkiye-specific experience, the paper notes both a "success" narrative attributed to accurate pre-characterization and precautions (Karahan, Gokceoglu 2025) and a "failure" narrative where unexpected conditions contributed to major TBM problems (Gokceoglu *et al*. 2022). Therefore, while MPAD does not explicitly separate within-class errors from class-crossing errors, reducing MPAD should, statistically and operationally, reduce the likelihood of disruptive class transitions and the downstream need for redesign.

The study uses the absolute percentage difference, so optimistic and conservative errors contribute equally to MPAD. From a construction risk viewpoint, optimistic errors can be more critical because they may lead to under-designed support; the case literature summarized in the manuscript illustrates how unexpected deterioration mechanisms and groundwater effects can trigger damage or collapse even when investigations exist (e.g., Alija *et al*. 2014; Aygar, Gokceoglu 2020). Nevertheless, for the paper's objective, absolute deviation is appropriate because it prevents positive and negative errors from cancelling out. This design choice is consistent with the manuscript's uncertainty-quantification emphasis (Miranda *et al*. 2009; Pandit *et al*. 2019) and its framing of uncertainty as an unavoidable feature to be managed rather than eliminated (Spross *et al*. 2020).

Even without converting MPAD into direct economical values, the results carry clear planning implications. The dataset shows a right-skewed uncertainty profile (mean MPAD 16.82%, median 9.00%, and 53.6% of sections achieving MPAD < 10%, with bootstrap CIs reported in Table 1), implying that a subset of tunnel sections can exhibit disproportionately high mismatch and hence disproportionately high risk of construction disruption. The most striking example in Table 2 is the Yüksekova T-1 section, where MPAD reaches 73.05% (left tube) under comparatively low LDn (~ 0.13) and very low TCRn (~ 1.92) and RQDn (~ 0.94), consistent with the study's emphasis that complex geology plus limited investigation increases uncertainty. Methodologically, the study argues that structural geology controls are essential and that insufficient drilling along the alignment undermines model realism (Carter, Barnett 2022). This supports the practical interpretation that investing in investigation quality/coverage is not merely "more data," but specifically improves the structural-geological input needed for a credible model. The 2D partial dependence "decision maps" (Fig. 11) convert this into prescriptive guidance: to maintain a commonly useful precision target of MPAD ≈ 10%, the model indicates a combined threshold around TCRn > 12.5 with LDn > 0.35, and, in poorer rock masses (lower RQDn), an even stronger sensitivity to core recovery is implied. This is consistent with the wider literature considered in the study that aims to reduce uncertainty through better modelling and data integration (Fookes 1997; Boyd *et al*. 2020; Dong *et al*. 2015; Ertharter *et al*. 2023; Fang *et al*. 2024; Madsen *et al*. 2022).

A key methodological finding is that the relationship between IID indicators and MPAD is partly non-linear**.** Linear baselines (parsimonious OLS and Elastic Net) showed limited explanatory power (LOOCV $R^2 \approx 0.155–0.157$), whereas the Ran-

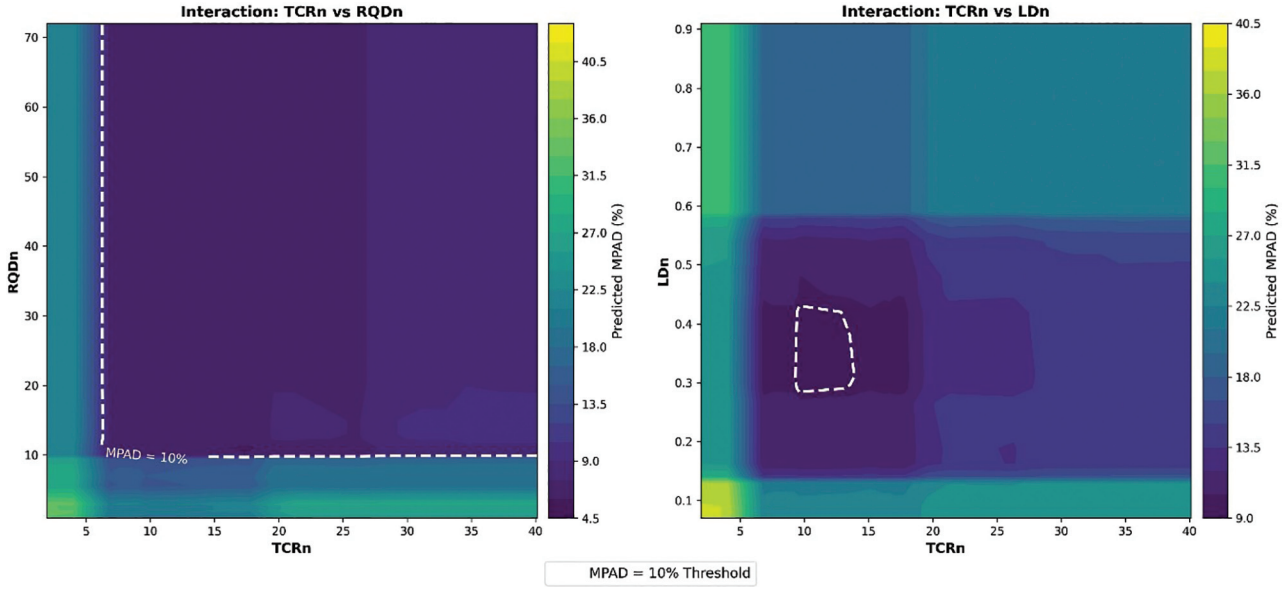

Fig. 11 2D Partial Dependence Plots (2D-PDP) showing the interaction effects of investigation indicators on MPAD. The white dashed contour lines represent the critical engineering threshold of MPAD = 10%

dom Forest substantially improved generalization (LOOCV $R^2 \approx 0.601$, OOB ≈ 0.55) and passed a permutation significance test ($p = 0.002$). This supports the manuscript's claim that interaction effects and threshold-like behaviour matter in practice, which is why ensemble learning provides better predictive utility for MPAD. In the RF feature hierarchy, RQDn, TCRn, and LDn collectively contribute 90% of importance, while UCSn is comparatively small (10%). Within the paper's framing, this implies that drilling coverage and core recovery/quality dominate uncertainty reduction more than increasing the frequency of UCS testing alone, consistent with the idea that limited borehole data can fundamentally impair ground-condition prediction (Yu, Mooney 2023). Finally, the study's multicollinearity diagnostics (VIF < 5) and the use of regularization (Elastic Net) strengthen confidence that these conclusions reflect a stable signal in the dataset rather than an artifact of correlated predictors.

CONCLUSIONS

The conclusions obtained from the study can be drawn as follows:

(a) The present study quantifies the discrepancy between rock mass classifications predicted during the tunnel investigation phase and those determined from lithological units encountered at the excavation face during construction. This discrepancy is expressed using the Mean Percent Absolute Difference (MPAD).

(b) The dataset contains 28 tunnel sections (left/right tubes) from 14 tunnels, enabling a robust statistical evaluation of how investigation-phase intensity and quality indicators influence MPAD. The predictors considered were the normalized investigation indicators LDn, TCRn, RQDn, and UCSn.

(c) A multi-layered and overfitting-aware statistical framework was implemented. First, potential multicollinearity among predictors was assessed (VIF values < 5 for all predictors), and then model structures were evaluated using both parsimonious linear baselines and regularized/non-linear models. Specifically, (i) parsimonious OLS models were selected using AIC/BIC, (ii) Elastic Net was applied to stabilize coefficients under correlated predictors, and (iii) Random Forest was used as a complementary model to capture non-linear interactions. Model performance was evaluated using LOOCV/Nested CV to provide unbiased generalization estimates. The statistical robustness of the final model was confirmed via permutation testing ($p = 0.002$), demonstrating that the observed predictive performance is highly unlikely to have occurred by chance.

(d) The comparative performance assessment shows that linear models (OLS and Elastic Net) provide limited explanatory power for MPAD, whereas the Random Forest model substantially improves predictive accuracy, achieving a LOOCV R^2 of 0.601 and an RMSE of 11.28. This indicates that the relationship between investigation indicators and MPAD is partly non-linear, and therefore benefits from ensemble-based modelling.

(e) Feature-importance results derived from the validated Random Forest model indicate that RQDn, TCRn, and LDn are the dominant contributors to MPAD prediction, while UCSn plays a comparatively smaller role. This finding implies that improving drilling coverage (LDn) and core recovery/quality (TCRn) is more influential for reducing investigation–construction discrepancy than increasing the number of UCS tests alone.

(f) Based on the interaction analysis using 2D-PDP, the study provides quantitative investigation intensity thresholds for tunnel planning. To achieve a standard engineering precision of MPAD < 10%, a balanced investigation strategy is required, with a minimum drilling density of LDn > 0.35 and a core recovery quality of TCRn > 12.5. These thresholds serve as a practical benchmark for determining the minimum borehole density and investigation quality needed to control geological uncertainty in similar rock mass conditions.

ACKNOWLEDGMENTS

This study is produced from the PhD thesis of the first author, Recep Temiz. Other two authors of the study are co-supervisor and supervisor of the PhD thesis. Special thanks is expressed to the anonymous reviewers for their valuable comments which improved the quality of manuscript.

Author contributions: Conceptualization, R.T. and C.G.; methodology, R.T. and E.B.A.; software, R.T.; validation, R.T., E.B.A. and C.G.; formal analysis, R.T.; investigation, R.T. and E.B.A.; resources, R.T. and G.G.; data curation, R.T.; writing–original draft preparation, R.T. and E.B.A.; writing–review and editing, C.G.; visualization, R.T. and E.B.A.; supervision, E.B.A. and C.G.; project administration, C.G. All authors have read and agreed to the published version of the manuscript.

Funding: This research received no external funding.

Conflicts of Interest: The authors declare no conflicts of interest. ChatGPT was used for the coding required for the statistical analyses performed in this study.

Abbreviations

LDn	The ratio of drilling length to tunnel length
TCRn	The ratio of the arithmetic mean of the TCR (total core recovery) values to tunnel length
RQDn	The ratio of the arithmetic mean of the RQD (rock quality designation) values to tunnel length
UCSn	The ratio of the arithmetic mean of the number of UCS (uniaxial compressive strength) test to tunnel length
MPAD	Mean percent absolute difference

REFERENCES

Alija, S., Torrijo, F.J., Quinta-Ferreira, M. 2014. Study of the unexpected collapse of the Ampurdán tunnel (Spain) using a finite elements model. *Bulletin of Engineering Geology and the Environment 73(2)*, 451–463.

Apostolaki, S., Karahan, S., Riga, E., Grigorios, T., Gokceoglu, C., Pitilakis, K. 2025. Seismic performance of tunnels and verification of available seismic risk models for the 2023 Kahramanmaraş earthquakes. *Tunnelling and Underground Space Technology 156*, 106185. https://doi.org/10.1016/j.tust.2024.106185

Aygar, E., Gokceoglu, C. 2020. Support system for Oceli highway tunnel excavated in fault zone (Ordu Ring Road Project, Turkey). In: *ISRM International Symposium Eurock 2020 – Hard Rock Engineering, Trondheim, Norway, 14–19 June. Paper Number:* ISRM-EUROCK-2020-188.

Aygar, E.B., Gokceoglu, C. 2021. Effects of Portal Failure on Tunnel Support Systems in a Highway Tunnel. *Geotechnical and Geological Engineering 39*, 5707–5726. https://doi.org/10.1007/s10706-021-01859-z

Benardos, A.G., Kaliampakos D.C. 2017. A methodology for assessing geotechnical hazards for TBM tunnelling- illustrated by the Athens Metro, Greece. *International Journal of Rock Mechanics and Mining Sciences 41(6)*, 987–999. https://doi.org/10.1016/j.ijrmms.2004.03.007

Bjureland, W., Spross, J., Johansson, F., Prästings, A., Larsson, S. 2017. Reliability aspects of rock tunnel design with the observational method. *International Journal of Rock Mechanics and Mining Sciences 98*, 102–110. https://doi.org/10.1016/j.ijrmms.2017.07.004

Boyd, L.D., Walton, G., Whitney, T.-G. 2020. Geostatistical estimation of Ground Class prior to and during excavation for the Caldecott Tunnel Fourth Bore Project. In: *Tunnelling and Underground Space Technology 100*, 103391, https://doi.org/10.1016/j.tust.2020.103391.

Can, A., Baskose, Y., Gokceoglu, C. 2022. Stability assessments of a triple-tunnel portal with numerical analysis (south of Turkey). *Geotechnical Research 40*, 1–13.

Carter, T.G., Barnett, W.P. 2022. Improving Reliability of Structural Domaining for Engineering Projects. *Rock Mechanics and Rock Engineering 55*, 2523–2549. https://doi.org/10.1007/s00603-021-02544-6

Çoruh, E., Köksal, A.O., Kaplan, C., Demirci, M. 2017. Kop Tüneli Yapım Çalışmaları ve Metodolojisi. *Ordu Üniversitesi Bilim ve Teknoloji Dergisi 7(2),* 275–288 [In Turkish].

Dong, M., Neukum, C., Hu, H., Azzam, R. 2015. Real 3D geotechnical modeling in engineering geology: a case study from the inner city of Aachen, Germany. *Bulletin of Engineering Geology and the Environment 74*, 281–300.

Erharter, G.H., Weil J., Bacher L., Heil F., Kompolschek, P. 2023. Building information modelling based ground modelling for tunnel projects – Tunnel Angath/ Austria. *Tunnelling and Underground Space Technology 135*, 105039, https://doi.org/10.1016/j.tust.2023.105039

Fang, G., Nilot, E.A., Li, Y.E., Tan, Y.Z., Cheng, A. 2024. Bayesian updating of tunneling risk predictions using continuous seismic data: Applications in urban tunneling. *Tunnelling and Underground Space Technology 147*, 105702.

Fellin, W., Lessmann, H., Oberguggenberger, M., Vieider, R. 2010. Analyzing risk in engineering: A probabilistic approach. *Structural Safety 32(6)*, 425–436.

Fookes, P.G. 1997. Geology for Engineers: the Geological Model, Prediction and Performance. In: *The Quarterly Journal of Engineering Geology 30(4)*, (November), 293–424.

Fortsakis, P., Nikas, K., Marinos, V., Marinos, P. 2012. Anisotropic behaviour of stratified rock masses in tunnelling. *Engineering Geology 141–142*, 74–83.

Gangrade, R.M., Grasmick, J.G., Mooney, M.A. 2022. Probabilistic assessment of void risk and grouting volume for tunneling applications. *Rock Mechanics and Rock Engineering 55,* 2771–2786.

Gokceoglu, C., Aygar, E.B., Nefeslioglu, H.A., Karahan, S., Gullu, S. 2022. A Geotechnical Perspective on a Complex Geological Environment in a High-Speed Railway Tunnel Excavation (A Case Study from Türkiye). *Infrastructures 7,* 155. https://doi.org/10.3390/infrastructures7110155

Goodman, R.E. 1995. Block theory and its application. *Geotechnique 45(3),* 383–423. https://doi.org/10.1680/geot.1995.45.3.383

Hack, R., Price, D., Rengers, N. 2006. A new approach to rock slope stability – a probability classification (SSPC). *Bulletin of Engineering Geology and the Environment 65(2),* 169–184.

Hao, K., Zhang, L., Zhou, C. 2018. A probabilistic approach for assessing the stability of rock slopes with correlated variables. *Arabian Journal of Geosciences 11(2)*, 2648.

Hao, Y., Rong, X., Ma, L., Fan, P., Lu, H. 2016. Uncertainty analysis on risk assessment of water inrush in karst tunnels. *Mathematical Problems in Engineering 2016*. Article ID 2947628, 11 pages.

Hong, Q., Lai, H., Liu, Y., Chen, R., Liu, C., Xie, J. 2021. Deformation control method of a large cross-section tunnel overlaid by a soft-plastic loess layer: A case study. *Bulletin of Engineering Geology and the Environment 80(5),* 4721–4730.

Huang, H., Zhang, D., Hu, H. 2016. Deformational responses of operated shield tunnel to extreme surcharge: A case study. *Structure and Infrastructure Engineering 12(3),* 354–367.

Isaksson, T., Stille, H. 2005. Model for Estimation of Time and Cost for Tunnel Projects Based on Risk Evaluation. *Rock Mechanics and Rock Engineering 38*, 373–398. https://doi.org/10.1007/s00603-005-0048-5

Karahan, S., Gokceoglu, C. 2025. Assessment for shallow and large tunnel construction in weak ground conditions: Application of tunnel boring machines. *Deep Underground Science and Engineering 4,* 132–148. https://doi.org/10.1002/dug2.12083

Karahan, S., Posluk, E., Buyukdemirci, F.B., Gokceoglu, C. 2025. Re-design of a railway tunnel intersected by surface rupture of the Erkenek fault segment during the 6 February 2023 Pazarcik (Mw 7.7) Earthquake (Türkiye). *Bulletin of Engineering Geology and the Environment 84,* 198. https://doi.org/10.1007/s10064-025-04217-y

Komu, M.P., Guney, U., Kilickaya, T.E., Gokceoglu, C. 2020. Using 3D numerical analysis for the assessment of tunnel – landslide relationship: Bahce–Nurdag tunnel (south of Turkey). *Geotechnical and Geological Engineering 38,* 1237–1254.

Langford, J.C., Diederichs, M.S. 2015. Quantifying uncertainty in Hoek–Brown intact strength envelopes. *International Journal of Rock Mechanics and Mining Sciences 74,* 91–102. https://doi.org/10.1016/j.ijrmms.2014.12.008

Li, S., Li, S., Zhang, Q., Xue, Y., Liu, B., Su, M., Wang, Z., Wang, S. 2010. Predicting geological hazards during tunnel construction. *Journal of Rock Mechanics and Geotechnical Engineering 2(3),* 232–242. https://doi.org/10.3724/SP.J.1235.2010.00232

Li, X., Li, X.B., Zhou, Z.L., Su, Y.H., Cao, W.G., 2021. A non-probabilistic information-gap approach to rock tunnel reliability assessment under severe uncertainty. *Computers and Geotechnics 132,* 103940. https://doi.org/10.1016/j.compgeo.2020.103940

Liu, D., Zhang, D., Zhang, C., Zhang, L. 2020. Structural responses of shield tunnel under differential settlement caused by leakage: A case study. *Tunnelling and Underground Space Technology 103*, Article 103471.

Madsen, R.B., Høyer, A.-S., Andersen, L.T., Møller, I., Hansen, T.M. 2022. Geology-driven modeling: A new probabilistic approach for incorporating uncertain geological interpretations in 3D geological modeling. *Engineering Geology 309*, Article ID 106833.

Mahmoodzadeh, H., Moosavi, M., Ghasemi, H. 2021. A novel probabilistic approach for risk assessment in mechanized tunneling projects. *Soft Computing 25(6)*, 5006–5022.

Mahmoodzadeh, H., Moosavi, M., Ghasemi, H., 2022. A hybrid approach for probabilistic risk assessment of tunnel construction projects. *Geotechnical and Geological Engineering 40(3)*, 2803–2820.

Merrie, M. 2009. Trials and Tribulations – An Overview of slurry tunnelling in challenging ground conditions. *Proceedings of Underground Singapore 2009,* 12–32.

Miranda, T., Correia, A.G., Ribeiro e Sousa, L. 2009. Bayesian methodology for updating geomechanical parameters and uncertainty quantification. *International Journal of Rock Mechanics and Mining Sciences 46(7)*, 1144–1153. https://doi.org/10.1016/j.ijrmms.2009.03.008

Pandit, B., Tiwari, G., Latha, G.M., Babu, G.L.S. 2019. Probabilistic Characterization of Rock Mass from Limited Laboratory Tests and Field Data: Associated Reliability Analysis and Its Interpretation. *Rock Mechanics and Rock Engineering 52*, 2985–3001. https://doi.org/10.1007/s00603-019-01780-1

Panthi, K.K., Nilsen, B. 2007. Uncertainty analysis of tunnel squeezing for two tunnel cases using the convergence-confinement approach. *Tunnelling and Underground Space Technology 22(1)*, 3–21.

Perello, P. 2011. Estimate of the Reliability in Geological Forecasts for Tunnels: Toward a Structured Approach. *Rock Mechanics and Rock Engineering 44*, 671–694. https://doi.org/10.1007/s00603-011-0164-3

Sarna, S., Gutierrez, M., Mooney, M., Zhu, M. 2022. Predicting upcoming collapse incidents during tunneling in rocks with continuation length based on influence zone. *Rock Mechanics and Rock Engineering 55*, 5905–5931. https://doi.org/10.1007/s00603-022-02971-z

Seo, Y., Macias, F.J., Jakobsen, P.D., Bruland, A. 2018. Influence of Subjectivity in Geological Mapping on the Net Penetration Rate Prediction for a Hard Rock TBM. *Rock Mechanics and Rock Engineering 51*, 1599–1613. https://doi.org/10.1007/s00603-018-1408-2

Spross, J., Stille, H., Johansson, F., Palmstrom, A. 2020. Principles of Risk-Based Rock Engineering Design. *Rock Mechanics and Rock Engineering 53*, 1129–1143. https://doi.org/10.1007/s00603-019-01962-x

Thum, L., De Paoli, R. 2015. 2D and 3D GIS- based geological and geomechanical survey during tunnel excavation. *Engineering Geology 192*, 19–25.

Xiong, W., Zhang, L., Zhou, W. 2018. Probabilistic analysis of tunnel stability in spatially variable soils using the random finite element method. *Tunnelling and Underground Space Technology 71*, 664–678.

Ye, G.-L., Zhang, D., Zhang, L., Zhang, N. 2015. Mechanism of unusual settlement due to improper backfill grouting in DOT shield tunnelling. *Tunnelling and Underground Space Technology 49*, 79–91.

Yousuf, M., Ameen, D., Chanouria, R. 2025. Applications of NATM in Himalayan Tunneling: Innovative Strategies to Tackle Geological Complexities and Construction Challenges. *Indian Geotechnical Journal.* https://doi.org/10.1007/s40098-025-01334-z

Yu, H., Mooney, M. 2023. Characterizing the as-encountered ground condition with tunnel boring machine data using semi-supervised learning. *Computers and Geotechnics 154,* 105159. https://doi.org/10.1016/j.compgeo.2022.105159

Yum, S.-G., Ahn, S., Bae, J., Kim, J.-M. 2020. Assessing the Risk of Natural Disaster-Induced Losses to Tunnel-Construction Projects Using Empirical Financial-Loss Data from South Korea. *Sustainability12(19),* 8026.